Journal of Composites for Construction

EFFECT OF SPIRAL SPACING AND CONCRETE STRENGTH ON BEHAVIOR OF GFRP-REINFORCED HOLLOW CONCRETE COLUMNS

--Manuscript Draft--

Manuscript Number:	CCENG-2684R1
Full Title:	EFFECT OF SPIRAL SPACING AND CONCRETE STRENGTH ON BEHAVIOR OF GFRP-REINFORCED HOLLOW CONCRETE COLUMNS
Manuscript Region of Origin:	AUSTRALIA
Article Type:	Technical Paper
Manuscript Classifications:	63: Columns; 25: Bars; 319: Reinforced concrete
Funding Information:	
Abstract:	Hollow concrete columns (HCCs) are one of the preferred construction systems for bridge piers, piles, and poles because they require less material and have a high strength-to-weight ratio. While spiral spacing and concrete compressive strength are two critical design parameters that control HCC behavior, the deterioration of steel reinforcement is becoming an issue for HCCs. This study explored the use of glass-fiber-reinforced-polymer (GFRP) bars as longitudinal and lateral reinforcement in hollow concrete columns and investigated the effect of various spiral spacing and different concrete compressive strengths (fc'). Seven hollow concrete columns with inner and outer diameters of 90 mm and 250 mm, respectively, and reinforced with six longitudinal GFRP bars were prepared and tested. The spiral spacing was no spirals, 50 mm, 100 mm, and 150 mm; the fc' varied from 21 to 44 MPa. Test results show that reducing the spiral spacing resulted in increased HCC uniaxial compression capacity, ductility, and confined strength due to the high lateral confining efficiency. Increasing fc', on the other hand, increased the axial-load capacity but reduced the ductility and confinement efficiency due to the brittle behavior of high compressive-strength concrete. The analytical models considering the axial-load contribution of the GFRP bars and the confined concrete core accurately predicted the post-loading behavior of the HCCs.
Corresponding Author:	Allan Manalo, PhD, M.Eng, BSCEng University of Southern Queensland Toowoomba, Queensland AUSTRALIA
Corresponding Author E-Mail:	manalo@usq.edu.au
Order of Authors:	Omar S. AlAjarmeh
	Allan Manalo, PhD, M.Eng, BSCEng
	Brahim Benmokrane
	Warna Karunasena
	Priyan Mendis
Additional Information:	
Question	**Response**
Authors are required to attain permission to re-use content, figures, tables, charts, maps, and photographs for which the authors do not hold copyright. Figures created by the authors but previously published under copyright elsewhere may require permission. For more information see http://ascelibrary.org/doi/abs/10.1061/978	No

0784479018.ch03. All permissions must be uploaded as a permission file in PDF format. Are there any required permissions that have not yet been secured? If yes, please explain in the comment box.	
ASCE does not review manuscripts that are being considered elsewhere to include other ASCE Journals and all conference proceedings. Is the article or parts of it being considered for any other publication? If your answer is yes, please explain in the comments box below.	No
Is this article or parts of it already published in print or online in any language? ASCE does not review content already published (see next questions for conference papers and posted theses/dissertations). If your answer is yes, please explain in the comments box below.	No
Has this paper or parts of it been published as a conference proceeding? A conference proceeding may be reviewed for publication only if it has been significantly revised and contains 50% new content. Any content overlap should be reworded and/or properly referenced. If your answer is yes, please explain in the comments box below and be prepared to provide the conference paper.	No
ASCE allows submissions of papers that are based on theses and dissertations so long as the paper has been modified to fit the journal page limits, format, and tailored for the audience. ASCE will consider such papers even if the thesis or dissertation has been posted online provided that the degree-granting institution requires that the thesis or dissertation be posted. Is this paper a derivative of a thesis or dissertation posted or about to be posted on the Internet? If yes, please provide the URL or DOI permalink in the comment box below.	No
Each submission to ASCE must stand on its own and represent significant new information, which may include disproving	No

the work of others. While it is acceptable to build upon one's own work or replicate other's work, it is not appropriate to fragment the research to maximize the number of manuscripts or to submit papers that represent very small incremental changes. ASCE may use tools such as CrossCheck, Duplicate Submission Checks, and Google Scholar to verify that submissions are novel. Does the manuscript constitute incremental work (i.e. restating raw data, models, or conclusions from a previously published study)?	
Authors are expected to present their papers within the page limitations described in <u><i>Publishing in ASCE Journals: A Guide for Authors</u></i>. Technical papers and Case Studies must not exceed 30 double-spaced manuscript pages, including all figures and tables. Technical notes must not exceed 7 double-spaced manuscript pages. Papers that exceed the limits must be justified. Grossly over-length papers may be returned without review. Does this paper exceed the ASCE length limitations? If yes, please provide justification in the comments box below.	No
All authors listed on the manuscript must have contributed to the study and must approve the current version of the manuscript. Are there any authors on the paper that do not meet these criteria? If the answer is yes, please explain in the comments.	No
Was this paper previously declined or withdrawn from this or another ASCE journal? If so, please provide the previous manuscript number and explain what you have changed in this current version in the comments box below. You may upload a separate response to reviewers if your comments are extensive.	Yes
Please provide the previous manuscript number and explain what you have changed in this current version in the comments box below. You may upload a separate response to reviewers if your comments are extensive.	MS CCENG-2666. The editor required the following information, which are now included in the revised manuscript (lines 112-116). a) Cross-sectional area of the FRP bar by immersion testing. b) Bar area used in the calculation of tensile stress (which affects strength and modulus)

as follow-up to "Was this paper previously declined or withdrawn from this or another ASCE journal? If so, please provide the previous manuscript number and explain what you have changed in this current version in the comments box below. You may upload a separate response to reviewers if your comments are extensive."	
Companion manuscripts are discouraged as all papers published must be able to stand on their own. Justification must be provided to the editor if an author feels as though the work must be presented in two parts and published simultaneously. There is no guarantee that companions will be reviewed by the same reviewers, which complicates the review process, increases the risk for rejection and potentially lengthens the review time. If this is a companion paper, please indicate the part number and provide the title, authors and manuscript number (if available) for the companion papers along with your detailed justification for the editor in the comments box below. If there is no justification provided, or if there is insufficient justification, the papers will be returned without review.	This is a stand-alone paper.
If this manuscript is intended as part of a Special Issue or Collection, please provide the Special Collection title and name of the guest editor in the comments box below.	This submission is part of regular issue.
Recognizing that science and engineering are best served when data aremade available during the review and discussion of manuscripts andjournal articles, and to allow others to replicate and build on workpublished in ASCE journals, all reasonable requests by reviewers formaterials, data, and associated protocols must be fulfilled. If you are restricted from sharing your data and materials, please explain below.	All the materials and information contained in the paper are not restricted and are available to all.
Papers published in ASCE Journals must make a contribution to the core body of knowledge and to the advancement of the field. Authors must consider how their new knowledge and/or innovations add	This study is the first to explore the use of glass-fiber-reinforced-polymer (GFRP) bars as longitudinal and lateral reinforcement in hollow concrete columns and investigated the effect of various spiral spacing and different concrete compressive strengths. This paper provides an understanding of the behavior of a new construction system to

value to the state of the art and/or state of the practice. Please outline the specific contributions of this research in the comments box.	help narrow the current knowledge gap related to using GFRP bars as internal reinforcement in concrete compressive members. It also provides additional data for establishing design guidelines and specifications on the use of GFRP reinforcement in hollow concrete columns.
The flat fee for including color figures in print is $800, regardless of the number of color figures. There is no fee for online only color figures. If you decide to not print figures in color, please ensure that the color figures will also make sense when printed in black-and-white, and remove any reference to color in the text. Only one file is accepted for each figure. Do you intend to pay to include color figures in print? If yes, please indicate which figures in the comments box.	No
If there is anything else you wish to communicate to the editor of the journal, please do so in this box.	The authors would like to thank the Editor and reviewers for their efforts and time in reviewing the paper. The comments will surely enhance and add to the paper. The authors have attempted to respect and answer the editor's comments.

EFFECT OF SPIRAL SPACING AND CONCRETE STRENGTH ON BEHAVIOR OF GFRP-REINFORCED HOLLOW CONCRETE COLUMNS

Omar S. AlAjarmeh[1], Allan C. Manalo[2,*], Brahim Benmokrane[3], Warna Karunasena[4], and Priyan Mendis[5]

Abstract

Hollow concrete columns (HCCs) are one of the preferred construction systems for bridge piers, piles, and poles because they require less material and have a high strength-to-weight ratio. While spiral spacing and concrete compressive strength are two critical design parameters that control HCC behavior, the deterioration of steel reinforcement is becoming an issue for HCCs. This study explored the use of glass-fiber-reinforced-polymer (GFRP) bars as longitudinal and lateral reinforcement in hollow concrete columns and investigated the effect of various spiral spacing and different concrete compressive strengths (f_c'). Seven hollow concrete columns with inner and outer diameters of 90 mm and 250 mm, respectively, and reinforced with six longitudinal GFRP bars were prepared and tested. The spiral spacing was no spirals, 50 mm, 100 mm, and 150 mm; the f_c' varied from 21 to 44 MPa. Test results show that reducing the spiral spacing resulted in increased HCC uniaxial compression capacity, ductility, and confined strength due to the high lateral confining efficiency. Increasing f_c', on the other hand, increased the axial-load capacity but reduced the ductility and confinement efficiency due to the brittle behavior of high compressive-strength concrete. The analytical models considering the axial-load contribution of the GFRP bars and the confined concrete core accurately predicted the post-loading behavior of the HCCs.

Keywords: Hollow column; GFRP bar; Spiral pacing; Concrete Compressive Strength.

[1]PhD Candidate, University of Southern Queensland, Centre for Future Materials (CFM), School of Civil Engineering and Surveying, Toowoomba 4350, Australia. E-mail: omar.alajarmeh@usq.edu.au

[2]Associate Professor of Structural Engineering, University of Southern Queensland, School of Civil Engineering and Surveying, Centre for Future Materials (CFM), Toowoomba, QLD 4350, Australia. E-mail: allan.manalo@usq.edu.au

[3]Professor of Civil Engineering, University of Sherbrooke, Department of Civil Engineering, Sherbrooke, Quebec, Canada. Email: Brahim.Benmokrane@USherbrooke.ca

[4]Professor of Structural Engineering, University of Southern Queensland, School of Civil Engineering and Surveying, Centre for Future Materials (CFM), Toowoomba, QLD 4350, Australia. E-mail: karu.karunasena@usq.edu.au

[5]Professor in the Department of Infrastructure Engineering, The University of Melbourne, Department of Infrastructure Engineering, Victoria 3010, Australia. Email: pamendis@unimelb.edu.au

INTRODUCTION

Hollow concrete columns (HCCs) are one of the preferred construction systems in civil infrastructures—including bridge piers, ground piles, and utility poles—to minimize the overall weight and reduce costs given the small amount of concrete in the column itself and the underlying foundations. HCCs are also considered a practical solution to increase the strength-to-mass ratio of structures compared to the solid concrete columns (Lignola, et al., 2007, Kusumawardaningsih and Hadi, 2010, Hadi and Le, 2014, Lee, et al., 2015). Designing an HCC with sufficient strength and reliable structural performance, however, requires careful consideration of some critical parameters, including lateral-reinforcement details and concrete compressive strength (Zahn, et al., 1990, Mo, et al., 2003, Lignola, et al., 2007, Lee, et al., 2015, Liang, et al., 2015). Lignola, et al. (2011) stated that providing widely spaced lateral reinforcement (greater than 400 mm) in HCCs leads to brittle failure, premature longitudinal-bar buckling, and decreased ductility. On the other hand, Lee, et al. (2015) indicated that reducing the lateral-reinforcement spacing from 80 mm to 40 mm increased ductility by 20% and minimized the damage in the inner concrete core. In addition, Mo, et al. (2003) found that increasing the concrete compressive strength from 30 MPa to 50 MPa yielded stiffer compression resistance in HCC, but with up to a 50% reduction in deformation capacity due to faster crack propagation and easier concrete splitting. Based on these studies, it can be concluded that the deformation capacity of steel-reinforced HCCs is significantly affected by lateral-reinforcement details, while their mode of failure is associated with concrete compressive strength.

In aggressive environments, the steel reinforcement in concrete columns is highly vulnerable to corrosion, leading to the development of a rusted shell around the reinforcement and its expansion of about 6 to 10 times its original volume (Verma, et al., 2014). This process initiates hairline cracks in the concrete that progress into wide cracks, which significantly reduces the ultimate axial capacity and leads to the brittle failure behavior of concrete columns owing to the damage to the lateral reinforcement (Pantelides, et al., 2013). Steel corrosion costs the Australian economy more than $13 billion per year (Cassidy, et al., 2015), while Canada and the US spend from $50 to 100 billion on repairing deteriorated concrete structures (Tannous, 1997; Manalo, et al., 2012). This issue has motivated many researchers around the world to investigate the use of high-strength and non-corroding reinforcement in building new concrete structures.

Fiber-reinforced-polymer (FRP) reinforcing bars are now becoming an effective alternative in concrete structures because of their non-corroding properties. FRP bars have also proven to be promising as longitudinal reinforcement in concrete columns due to them having higher strength and strain capacity than steel (Manalo, et al., 2014, Maranan, et al., 2018). In particular, glass-FRP (GFRP) bars are considered to be the most cost-effective, non-corroding composite reinforcing material (Benmokrane, et al., 1995). GFRP-reinforced solid concrete columns have been successfully tested and exhibited enhanced post-loading response (the response after spalling of the concrete cover) owing to the increased deformation capacity of the columns and adequate confined strength because of the high tensile strength of the lateral GFRP reinforcement (Pantelides, et al., 2013, Hadi, et al., 2016). Despite GFRP bars having lower elastic moduli than steel, Pantelides, et al. (2013) noted an improvement of 3% and 5% in the confined strength and ductility, respectively, of solid concrete columns due to the ineffectiveness of the steel reinforcement in providing confinement after yielding. Moreover, Hadi, et al. (2016) highlighted the benefit of using GFRP reinforcement instead of steel in solid concrete columns. Their comparison of the behavior of solid concrete columns reinforced with 6 pieces of 14.6 mm diameter longitudinal GFRP bars and other concrete columns with 6 pieces of 12.0 mm diameter steel bars showed that the GFRP-reinforced columns had 4% higher ductility than the steel-reinforced columns. In addition, the ductility of the GFRP-reinforced columns was further enhanced by up to 33% when the spacing between spirals was reduced from 60 mm to 30 mm. Similar to the case of steel-reinforced HCCs, these studies showed that both spiral spacing and concrete compressive strength are important design parameters that affect the behavior of solid columns reinforced with GFRP bars and spirals. It is therefore essential to determine the effects of these design parameters on the behavior of HCCs reinforced with GFRP bars. The significance of this work, on the other hand, lies with it extending previous attempts by (AlAjarmeh, et al., 2019a) and (AlAjarmeh, et al., 2019b) in investigating the effect of different inner-to-outer (i/o) diameter ratios and reinforcement ratios (ρ), respectively, of HCCs with GFRP reinforcement. The test results show that creating a hollow within the concrete columns changed their failure mode from brittle to a more ductile and progressive mode. In addition, an increase of 22% and 74% in the confined strength and ductility factor were observed. Moreover, they concluded that the increase in i/o ratio led to a gradual failure and more stability in the loading history. In contrast, increasing ρ increased the strength and significantly contributed to lateral confinement.

This study aimed at investigating the effectiveness of GFRP bars and spirals as internal reinforcement in HCCs. It focused on evaluating the effect of lateral spiral spacing and concrete compressive strength on the failure mode, load–deformation behavior, ductility, and confined strength of hollow concrete columns. Understanding the behavior of this new construction system will help narrow the current knowledge gap related to using GFRP bars as internal reinforcement in concrete compressive members, and will provide additional data for establishing design guidelines and specifications on the use of GFRP reinforcement in hollow concrete columns.

EXPERIMENTAL PROGRAM

Materials

Reinforcement

Grade III #5 GFRP bars with a 15.9 mm nominal diameter (CSA, 2012), as shown in Fig. 1(a), were used to reinforce the hollow concrete columns longitudinally. The transverse reinforcement was Grade III #3 GFRP spirals with a 9.5 mm nominal bar diameter and an inside diameter of 180 mm, as shown in Fig. 1(b). This type of transverse reinforcement was adopted as it provides higher lateral confinement to the concrete core compared to conventional circular hoops (Maranan, et al., 2016). The GFRP bars and spirals were manufactured by pultruding glass fibers impregnated with vinyl-ester resin, and then coating the outer surface with sand. Table 1 provides the physical and mechanical properties of the GFRP bars, as reported before by Benmokrane, et al. (2017) for the same reinforcements which were manufactured from the same production lot, denoted that the standard deviation values are included between brackets. As recommended by CSA S806 code (CSA, 2012), the tensile strength and modulus of elasticity of the GFRP bars were calculated using the nominal bar area. It should be noted that the mechanical properties in Table 1 are for straight bars and the ultimate tensile strength of spirals was calculated based on CSA S806 code (CSA, 2012).

Concrete

Four different levels of normal-strength concrete were cast in the column samples. One mix was a ready-mixed concrete with a maximum coarse aggregate size of 10 mm, slump of 103 mm, an average compressive strength (f_c') of 26.8 MPa, and a standard deviation (SD) of 3.54 MPa. In addition, two batches of concrete were mixed in the laboratory with a maximum aggregate size of 10 mm and slumps of 91 and 106 mm for the samples with f_c' of 36.8 MPa (SD of 1.56) and 44.0 MPa (SD of 2.31), respectively. The other concrete mix was post-mixed concrete (ready-packed dry mix) with a maximum aggregate size of 3 mm and slump of 110 mm, which gave an average f_c' of 21.2 MPa (SD of 3.12). The compressive strength of these concrete batches were measured by preparing six concrete cylinders 100 mm in diameter and 200 mm in height for each concrete mix based on ASTM C31 specification (ASTM C31, 2015) and tested on the day of column testing according to the procedures described in ASTM C39 specification (ASTM C39, 2015).

Specimen Details

Seven concrete columns fully reinforced with GFRP bars with overall dimensions of 250 mm in diameter and 1 m in height were cast and tested. The cross-section was determined based on the maximum capacity testing machine. On the other hand, the height-to-diameter ratio of the samples was 4, which ensured avoiding global buckling for the column samples as reported by Maranan, et al. (2016). All columns were longitudinally reinforced with six GFRP bars in accordance with the reinforcement details and ratio recommended in AS3600 code (AS3600, 2011) for steel reinforcement owing to the lack of codes and standards regarding the use of GFRP bars in compression. Consequently, the reinforcement ratio of 2.79% was similar for all test columns, calculated by dividing the total area of the longitudinal GFRP bars (A_{FRP})

(1,191 mm^2) by the gross cross-sectional area of the columns (A_g) (42,704 mm^2). Concrete columns were divided into two groups to investigate the effect of spiral spacing and concrete compressive strength:

- Group A: Three columns were reinforced laterally with GFRP spirals with a spacing of 50 mm, 100 mm, and 150 mm at the middle portion of the samples (500 mm). Another column without lateral reinforcement at the testing region (500 mm) was prepared to evaluate the effect of the lateral reinforcement. These lengths were chosen to ensure crushing failure in the bars with a length of 50 mm, 100 mm, and 150 mm and the bar buckling failure in the last sample, this finding was reported by Maranan, et al. (2016) who found that bar buckling failure occurred in bars with a length of more than 200 mm. While CSA S806 code (CSA, 2012) recommends a clear spacing between spirals of less than 85 mm for the tested columns, the biaxial stress distribution in HCCs compared to the triaxial stress distribution in solid concrete columns (AlAjarmeh, et al., 2019a) requires that the most effective spiral spacing for HCCs be determined.
- Group B: Four columns were cast with different concrete strengths (21.2, 26.8, 36.8, and 44.0 MPa) and tested. These levels of compressive strength were considered normal-strength concrete, as indicated in ACI 318-8 code (ACI, 2008). The reinforcement details for all columns were kept the same by the reinforcement ratio of 2.79% and 100 mm spacing between lateral spirals to determine the effect of varying concrete compressive strength. Moreover, the adopted reinforcement details resulted in a stable load-carrying behavior and a gradual failure of the concrete core after the spalling of the concrete cover (AlAjarmeh, et al., 2019a). Choosing different levels of normal-strength of concrete led to significant change in the compressive behavior for hollow concrete columns as reported by Mo, et al. (2003).

The top and bottom 250 mm of the height of all the columns were laterally reinforced with GFRP spirals at a closed spacing of 50 m to prevent stress-concentration failure at the column ends. The hollow section was created by inserting a 1 mm thick PVC pipe with an external diameter of 90 mm at the centre of the samples during casting. This resulted in a hollow concrete column with a constant inner-to-outer diameter ratio of 0.36, which was found to provide ductile behavior due to the progressive failure of the concrete cover, followed by crushing of the concrete core and longitudinal bars with no spiral failure (AlAjarmeh, et al., 2019a, AlAjarmeh, et al., 2019b). It is worth mentioning that Kusumawardaningsih and Hadi (2010) and Hadi and Le (2014) used an almost similar inner-to-outer diameter ratio for steel-reinforced hollow concrete columns due to precisely capture the behavior of hollowness by using this ratio.

Figure 2 shows the typical cross-section of the columns tested, while Table 2 provides the different volumetric ratios, spacing, and f_c'. The volumetric ratios were calculated by dividing the volume of one spiral by the concrete-core volume within one spiral pitch. Columns were designated as either A or B to represent the specimen group, followed by the spiral spacing, and the concrete compressive strength f_c'. For example, column A-100-26.8 is a GFRP-reinforced hollow column from Group A with 100 mm spacing between lateral spirals and with f_c' of 26.8 MPa. Column B-100-26.8, on the other hand, is a GFRP-reinforced hollow column from Group B with 100 mm spacing between lateral spirals and with f_c' of 26.8 MPa.

Test Setup and Instrumentation

A total of six electrical-resistance strain gauges were attached to each column to measure the strain during testing. Two 3 mm long strain gauges were glued onto longitudinal GFRP bars at mid-height and also two on spirals at mid-height. The last two gauges were 20 mm in length and glued on the outer surface of concrete at the column mid height to measure the axial strain. Figures 3(a) shows the location of the strain gauges. Steel clamps measuring 50 mm in width and 10 mm in thickness were used at the top and bottom of the columns, in addition to 3 mm thick neoprene cushions were used to prevent premature cracking and ensure that failure occurred in the test region (column mid-height). In addition, 3 mm thick neoprene cushions were placed on the top and bottom of the columns for uniform load distribution. Moreover, wire mesh was used to cover the specimen for safety purposes and to prevent projectile debris upon column failure. Afterwards, the columns were tested under monotonic concentric loading with a 2,000 kN hydraulic cylinder. The applied load was measured with a 2,000 kN load cell, and the axial deformation was recorded with a string pot, as shown in Fig. 3(b). Throughout testing, the load, strain, and axial deformation were recorded with the System 5000 data logger. Failure propagation was also carefully observed and video recorded during the entire loading regime.

BEHAVIOUR OF COLUMNS WITH VARIOUS SPIRAL SPACING

Failure Mode

Group A columns were tested under concentric compression load until failure. Lignola, et al. (2007) indicated that the general failure for hollow concrete columns reinforced with steel bars is controlled by bar buckling and concrete crushing with highly spaced lateral reinforcement. The hollow concrete columns tested in our study experienced different modes of failure owing to the GFRP bars having higher strength than the steel bars. Typically, the failure in all columns started as vertically spreading hairline cracks appearing on the outer concrete surface at advance loading levels. Once they appeared, the cracks propagated and widened, leading to different spalling features of the outer concrete cover, rupturing longitudinal GFRP bars, and damaging the concrete core, all of which are described in detail below.

- A-N/A-26.8: This column experienced explosive spalling and failing of both the concrete cover and core, producing large concrete pieces falling from specimen mid-height. Consequently, global buckling in the longitudinal GFRP bars without fracturing was observed, as shown in Fig. 4(a).

- A-150-26.8: Limited concrete cover spalling localized at mid-height occurred in this column. Lateral expansion of the perimeter at mid-height was noted after concrete-cover spalling, leading to final failure, as highlighted by rupturing of the longitudinal GFRP bars and massive damage to the concrete core, as shown in Fig. 4(b). No damage to the lateral spiral was observed.
- A-100-26.8: Concrete-cover spalling in this column was gradual and continued until the entire column was affected. Lateral spirals held the concrete core and longitudinal bars. Final failure was due to rupture in the longitudinal GFRP bars and crushing of the concrete core at mid-height without damage to the lateral spirals, as shown in Fig. 4(c).
- A-50-26.8: Gradual overall concrete-cover spalling was observed, followed by lateral expansion in the concrete core, which was confined by the GFRP spirals. Sequential rupture of longitudinal GFRP bars in different locations throughout the column's height and concrete crushing of the concrete at the bottom occurred caused by stress concentration, as shown in Fig. 4(d).

The different failure mechanisms after spalling of the concrete cover were due to lateral-reinforcement spacing. The above results indicate that the hollow concrete columns with narrower spiral spacing evidenced more progressive failure and less damage to the concrete core than the columns with wider spacing. Lee, et al. (2015) observed similar behavior with steel-reinforced hollow columns. This finding can be correlated to the unbraced length of the longitudinal GFRP bars, which tried to buckle with the application of the compressive load. In particular, the failure of the column without lateral reinforcement (A-N/A-26.8) was consistent with that of GFRP-reinforced solid concrete columns tested by Maranan, et al. (2016). In this case, the concrete cover and core experienced brittle and explosive failure due to the long unbraced length of the longitudinal GFRP bars. Narrow spiral spacing, however, stabilized the longitudinal GFRP bars and resulted in the column's progressive failure. For all spiral-reinforced columns, using GFRP reinforcement delayed final failure due to its higher axial deformation capacity compared to the steel-reinforced hollow concrete columns (Lignola, et al., 2007, Kusumawardaningsih and Hadi, 2010).

Load-Deformation Behavior

Spiral spacing affects the load–deformation, confined strength, and ductility behavior of hollow concrete columns reinforced with GFRP bars, as shown in Figure 5 and Table 3. As can be seen from Figure 5, all the columns had almost linear-elastic behavior up to the spalling of the concrete cover but with lower stiffness as the spiral spacing narrowed. Table 3 also provides the slope of the linear-elastic portion of the load–deflection curve, where the deformation is the axial displacement of the sample with respect to the original height of its top part. The lower axial stiffness for columns with narrower spiral spacing is due to the weaker plane between the outer concrete cover and the concrete core, creating a slender outer concrete shell. The columns with closer spiral spacing, however, had more stability than those columns with wider spiral spacing after concrete-cover spalling (post-loading behavior) owing to the better lateral confinement provided by the lateral reinforcement. Hadi, et al. (2016), Hadi, et al. (2017), and Maranan, et al. (2016) made similar observations. The spiral spacing also affected the first axial peak load of the hollow columns. This first peak load (P_{n1}), denoted by the solid black circle in Figure 5, represents the load carried by both the unconfined concrete and longitudinal GFRP bars. The hollow concrete columns with closer spiral spacing exhibited a higher load than the columns with wider spiral spacing. Column A-50-26.8 had the highest load capacity, specifically 1%, 8%, and 17% higher than columns A-100-26.8, A-150-26.8, and A-N/A-26.8, respectively. This increase in the axial-load capacity—even with the same cross-sectional area and longitudinal reinforcement ratio—emphasizes the positive contribution of the lateral confinement in preventing crack propagation in the concrete. This led to a good distribution of the tensile stress in the concrete cover, resulting in spalling along the column height, as shown in Figure 4.

While the spalling of the concrete cover after the uniaxial peak resulted in a drop of axial load, its level can be correlated to the spiral spacing. For the column without lateral reinforcement (A-N/A-26.8), the load dropped significantly, and the column was unable to carry more load. Providing spirals activated the lateral confinement at the load–deformation part after P_{n1}, so that columns A-50-26.8, A-100-26.8, and A-150-26.8 retained most of the applied load with only a 1%, 10%, and 7% reduction in P_{n1}, respectively. Karim, et al. (2016) made similar observations. After that point, the lateral expansion of the cracking concrete was restricted by the lateral spirals, allowing the column to continue resisting the applied load at the post-loading stage at which point the concrete cover no longer makes a load contribution. This load-carrying resistance was controlled by the column volumetric ratio (see Table 2), which prevented the concrete core from crushing and the unbraced length of the longitudinal bars from buckling and crushing. Because of the good confinement of the concrete core and longitudinal bars, column A-50-26.8 exhibited a second peak load (P_{n2}) and had a confined strength 29% higher than columns A-100-26.8 and A-150-26.8. P_{n2} can be traced by the cross (×) in Figure 5. Table 3 shows that columns A-100-26.8 and A-150-26.8 had almost similar maximum confined strength values (f'_{cc}), even with different spiral spacing. f'_{cc} was calculated by dividing P_{n2} by the concrete core area (A_{core}) with a diameter denoted by the distance between spiral centres. The axial strain of the GFRP bars was, however, 13% higher in column A-150-26.8 than in column A-100-26.8, suggesting that neither a spacing of 100 mm nor 150 mm was able to increase the confined strength of the concrete core. Moreover, the column with 50 mm spiral spacing made the concrete core to fail more progressively than columns A-100-26.8 and A-

150-26.8. This was due to the efficiency of the closer spirals in delaying the crack progression in the concrete core and in reducing the unbraced length of the longitudinal GFRP bars. This also accounts for the higher ductility of the columns with smaller spiral spacing. For instance, column A-50-26.8 had 30% and 50% higher ductility than columns A-100-26.8 and A-150-26.8, respectively. The ductility of the HCC was calculated as the ratio between ultimate deformation (Δ_u) (represents the deformation at the failure point) to the yield deformation (Δ_y) (represents the deformation at the level of the uniaxial load with respect to the extended linear-elastic line), as suggested by Cui and Sheikh (2010). In the HCCs herein, the lateral spiral reinforcement provided nonuniform confining stress along the column height, resulting in crack development in the concrete core at the unconfined region, i.e. between spirals, decreasing column capacity after P_{n2} [Figure 5]. Consequently, a narrower spiral spacing in the tested region yielded a longer descending part and the area under the load–deformation curve was larger than with the columns with wider spiral spacing, indicating that the column had higher toughness. Finally, columns A-50-26.8 and A-100-26.8 recorded a 7% and 2% higher failure load than A-150-26.8, since the closer spiral spacing protected the concrete core from sudden failure and gave the GFRP bars a chance to withstand greater axial loads.

Load–Strain Behavior

Figure 6 shows the load versus axial strain (negative sign) in the longitudinal GFRP bars and lateral strain (positive sign) in the spirals for Group A columns. These strain readings were taken as the average of the strain readings at longitudinal bars and spirals where the difference between the maximum and minimum strains did not exceed 5% of the average value. After the axial linear-elastic load–strain response, the columns started to show a nonlinear ascending part due to hairline cracks appearing in the concrete cover. Interestingly, the hairline cracks started to appear at a strain of around 1,500 $\mu\varepsilon$ measured by the strain gauges attached to the concrete. This value is similar to the concrete cracking limit reported by Saatcioglu and Razvi (1992).

This observation was further verified in column A-N/A-26.8, which failed after reaching this axial strain ($\varepsilon_{c,P_{n1}}$) [Table 3]. In fact, the narrower the spiral spacing, the higher the ultimate recorded axial concrete strain due to the delay in crack propagation and greater concrete-cover stability. For instance, a strain ($\varepsilon_{c,P_{n1}}$) of 1,455 $\mu\varepsilon$, 1,952 $\mu\varepsilon$, 2,162 $\mu\varepsilon$, and 2,524 $\mu\varepsilon$ was recorded in columns A-N/A-26.8, A-150-26.8, A-100-26.8, and A-50-26.8, respectively. In the longitudinal bars, the axial compressive-strain values at the first peak load ($\varepsilon_{b,P_{n1}}$) were 1,645 $\mu\varepsilon$, 3,902 $\mu\varepsilon$, 2,318 $\mu\varepsilon$, and 3,884 $\mu\varepsilon$ in columns A-N/A-26.8, A-150-26.8, A-100-26.8, and A-50-26.8, respectively. These strain values are between 7% and 17% of the ultimate tensile strain of the GFRP bars, suggesting that they contributed significantly to the uniaxial compression capacity of the columns. Consequently, their contribution should not be ignored, as indicated in the current design codes (CSA, 2012, ACI, 2015). It is also noteworthy to mention that the GFRP spirals recorded significant lateral strain only after the column's first peak load, indicating that the lateral reinforcement was activated and provided confinement only after the concrete cover spalled.

After the cover spalled (post-loading stage), the longitudinal GFRP bars continued carrying a load, and the strain of the lateral spirals increased dramatically due to dilation of the concrete core. It is important to note in Fig. 6 that the strains in the longitudinal GFRP bars and spirals in columns A-100-26.8 and A-150-26.8 plateaued in the post-loading stage, unlike column A-50-26.8 in which it continued to increase. This behavior indicates that the spiral spacing of 100 mm and 150 mm were adequate to prevent the bars from buckling but not to prevent or delay the initiation of cracks in the concrete core (Fig. 4). From this result, it can be deduced that effective confinement is related more to the concrete core rather than the longitudinal bars, since GFRP bars have linear-elastic behavior up to failure. This finding also explains the observed final failure in all hollow columns tested, in which the longitudinal GFRP bars ruptured at a strain of 10,548 $\mu\varepsilon$, 10,692 $\mu\varepsilon$, and 13,539 $\mu\varepsilon$ in columns A-150-26.8, A-100-

26.8, and A-50-26.8, respectively, as shown in Fig. 6. These strain levels ranged from 50.2% to 64.5% of the ultimate tensile strain of the GFRP bars. It is interesting to note that using a spiral spacing of 50 mm resulted in a 27% higher crushing strain of the GFRP bars than did 100 mm and 150 mm spacing. The average of these values matches the proposed average of 12,200 $\mu\varepsilon$ ±1,200 $\mu\varepsilon$ as the maximum compressive strain for GFRP bars suggested by Fillmore and Sadeghian (2018).

Figure 6 shows that increasing the spiral spacing increased the efficiency of concrete-core confinement and the longitudinal GFRP bars until failure. For instance, column A-150-26.8 recorded the lowest lateral strain of 4,542 $\mu\varepsilon$ at failure, since the widely spaced lateral spirals were unable to limit and delay crushing of the concrete core. On the other hand, column A-100-26.8 recorded 12,740 $\mu\varepsilon$ at failure, resulting in a higher deformation capacity as can be seen in Fig. 5, while column A-50-26.8 recorded 6,507 $\mu\varepsilon$. Although column A-100-26.8 had a higher lateral strain than column A-50-26.8, the latter had higher lateral confinement proportional to the vertical spacing between spirals. Finally, columns with closer spiral spacing showed higher engagement in terms of hoop stress in confining the concrete core proportional to the vertical spacing between spirals. Consequently, this study recommends the 50 mm spacing as lateral reinforcement for hollow concrete columns or the equivalent volumetric ratio to get significantly enhanced strength and ductility. The hoop stress was calculated by multiplying the spiral strain at the failure by its modulus of elasticity.

Volumetric Strain Behavior

Figure 7(a) shows the normalized first peak load for Group A columns. The normalized first peak load was calculated by dividing P_{n1} by the multiplication of gross cross-sectional area of the column and characterized concrete compressive strength ($f_c' \times A_g$). The figure shows that the normalized first peak load (P_{n1}) increased as the spacing between spirals narrowed. This is an interesting result as both the concrete strength and number of bars were the same for all columns. This finding indicates that the lateral confinement provided by the GFRP spirals contributed to the uniaxial compression capacity of the HCCs by preventing lateral plastic concrete dilation after the appearance of cracks and thereby enhancing the concrete’s compressive strength. This phenomenon can be explained by the volumetric strain (ε_v) or the dilation rate of the concrete, which is defined in Eq. (1) for solid concrete columns (Mirmiran and Shahawy, 1997).

$$\varepsilon_v = \varepsilon_c + 2\varepsilon_r \qquad \text{Eq. (1)}$$

where ε_c is the axial strain measured in the longitudinal GFRP bars and ε_r is the lateral strains measured in the GFRP spirals. This formula expresses the change of volume with respect to a unit volume in solid concrete columns loaded under a triaxial stress state. In a perfectly elastic condition for solid columns, the conventional slope of the ascending line between volumetric strain and axial strain is given as (1-2v) (Mohamed, et al., 2014), where v is the Poisson’s ratio of the concrete (equal to 0.2), as shown in Fig. 7(b). In this figure, positive ε_v represents volume reduction, whereas negative ε_v represents expansion. The curve’s deviation from the slope line represents crack initiation until the spalling of the concrete cover at ε_v. A similar slope for HCCs was obtained by modifying Eq. (1) by multiplying ε_r by 3 instead of 2 to attain a slope of (1-2v). This means that the lateral dilation of the concrete in HCCs is lower than in solid columns. This is because of the nonuniform distribution of biaxial stresses in HCCs, which causes a portion of the concrete dilation to be inward, as also indicated by Cascardi, et al. (2016) or referred to the higher stability in the concrete core due to use hollow section allowing to show higher axial-to-lateral strain ratio as reported by Lignola, et al. (2008). Moreover, based on the slope equation, the Poisson’s ratio for the tested columns was 0.18, which is within the typical range for normal-strength concrete (0.15–0.22) (Mohamed, et al., 2014). According to Fig. 7(b), the spiral spacing significantly affected concrete stability by delaying the elastic dilation of the concrete, as shown by the higher volumetric strain at the higher axial compressive strain.

BEHAVIOUR OF COLUMNS WITH DIFFERENT CONCRETE STRENGTH

Failure Mode

Group B columns, which had different concrete compressive strengths (f_c'), exhibited different failure modes in terms of spalling and the degree of damage of the concrete core. All, however, failed by the rupturing of longitudinal GFRP bars with the GFRP spirals remaining intact. Therefore, after the hairline cracks appeared on the outer concrete cover, column failure progressed as described below.

- B-100-21.2: Cracks extended at the bottom half of the column, leading to spalling of the concrete cover. The cracks then propagated to the middle portion and the concrete core. This resulted in crushing of the entire concrete core at mid-height, as shown in Fig. 8(a).
- B-100-26.8: Concrete-cover spalling in this column was gradual and continued until it affected the entire height, as shown in Fig. 8(b).
- B-100-36.8: Vertical cracks along the column height appeared, followed by overall spalling of the concrete cover. Partial degradation was observed in the concrete core at different locations, which resulted in the rupture of GFRP bars at these locations [Fig. 8(c)].
- B-100-44.0: Cracks extending and propagating at the mid-bottom half of the column height were observed, followed by splitting off of large concrete pieces at the outer concrete cover. Slow degradation in the concrete core resulted in the rupture of two longitudinal GFRP bars and loss of the concrete core, as shown in Fig. 8(d).

From the above observations, it can be concluded that increasing the f_c' changed the failure of HCCs reinforced with GFRP bars from ductile to brittle. This was clearly evidenced by column B-100-44.0, which failed abruptly after the whole concrete core degraded, with limited failure in the longitudinal bars. Consistent with Mo, et al. (2003), column B-100-44.0 showed faster spalling of the concrete cover as flakes, compared to the other columns, which exhibited gradual concrete spalling. More longitudinal GFRP bars ruptured in the columns with lower f_c', which can be attributed to the GFRP bars having a greater stiffness than the concrete, so the reinforcement carried more of the load after the concrete cover spalled. The localized concrete spalling in column B-100-21.2 can be explained by the smaller aggregate size (3 mm), which resulted in more micro-cracks between the concrete paste and the fine aggregate particles, which was also reported by Cui and Sheikh (2010).

Load–Deformation Behavior

The variation in f_c' (21.2 to 44.0 MPa) significantly affected the load–deformation behavior, confinement efficiency, and ductility of the tested HCCs. Figure 9 and Table 4 show that the use of higher concrete compressive strength resulted in stiffer load–deformation behavior because of the increase in the concrete's elastic modulus from 21.6 GPa (f_c' = 21.2 MPa) to 31.2 GPa (f_c' = 44 MPa). Predictably, increasing the f_c' increased the axial-load capacity at the first load peak (P_{n1}) of columns B-100-26.8, B-100-36.8, and B-100-44.0, respectively, by 31.1%, 73.1%, and 107.3% compared to column B-100-21.2. The insignificant deviation between these percentages with respect to the percentage increase of the concrete compressive strength can be related to concrete being a nonhomogeneous material that is affected by placing, compacting, and curing (Neville, 1995). The increase in f_c', however, decreased the contribution of the longitudinal GFRP bars owing to the increased concrete stiffness, which was getting closer to the GFRP-bar stiffness. The contribution of longitudinal GFRP bars to P_{n1} of columns B-100-21.2, B-100-26.8, B-100-36.8, and B-100-44.0 was 22.1%, 11.7%, 8.2%, and 6.9%, respectively. The axial load contribution of the GFRP bars was calculated by multiplying bar axial strain by bar elastic modulus and total bar area divided by P_{n1}. Cracks that widened and extended along the outer concrete cover resulted in a load reduction after P_{n1}, in which the magnitude of the drop in load capacity can be correlated to the f_c'. The load drop was 15.2%, 11.5%, 10.2%, and 4.1% for columns B-100-44.0, B-100-36.8, B-100-26.8, and B-100-21.2, respectively, which emphasizes the significant contribution of the concrete cover, especially for the columns with higher f_c'. This finding is consistent with Mo, et al. (2003), who observed a higher load drop in columns with higher f_c'. Addressing such an issue would involve using lower concrete-cover area to gross area or increasing the lateral reinforcement to mitigate the load drop after P_{n1}, as noticed in the Group A columns.

After the load drop (after P_{n1}), the Group B columns exhibited different post-loading behavior until the second axial peak load (P_{n2}). Note that P_{n2} is the contribution of the confined concrete core in addition to the longitudinal GFRP bars. Therefore, column H-100-44.0 showed higher load-deformation capacity and recorded P_{n2} 49.2% and 15.4% higher than columns B-100-26.8 and B-100-36.8, respectively. This was due to the former's higher f_c'. Figure 9 shows a slightly higher stiffness after the maximum load with increasing f_c', which is due to the strength enhancement in the post-loading stage, as reported by Morales (1982). This increase was not enough, however, to increase the confinement efficiency with respect to the unconfined concrete strength (f_{co}) of the columns. In fact, column B-100-44.0 showed 8.7% and 3.4% lower confinement efficiency than columns B-100-26.8 and B-100-36.8, respectively. This behavior can be explained by the significant load drop after the first axial peak load for the columns with high concrete compressive strength and emphasized the CSA S806 code (CSA, 2012) recommendation of using a high volumetric ratio for high f_c'.

In order to further evaluate the effect of the compressive strength of concrete for hollow columns reinforced with GFRP bars, the confinement efficiency (*C.E.*) was calculated from the ratio of confined strength (f'_{cc}) to the unconfined strength (f'_{co}) when the outer concrete surface was free of cracks ($0.85f'_c$). The confined concrete-core strength was calculated by dividing P_{n2} by the concrete-core area *(A_{core})*. The A_{core} was calculated based on the diameter measured from the lateral spiral centers, as was also implemented by Tobbi, et al. (2014). After P_{n2}, the load–deformation behavior continued to deteriorate until the longitudinal GFRP bars and concrete core recorded the final failure load (P_f) (Table 4). This strength degradation was caused by cracks developing in the concrete core, while the longitudinal GFRP bars were still intact and carrying the applied load. In the case of column B-100-21.2, the decrease in the slope of the load–deformation curve was due to the concrete core crushing, as initiated by the small aggregate size (3 mm) used and highlighted by the failure mode, leading to a wide load–deformation curve but without enhanced peak loads. Cui and Sheikh (2010) made similar findings, concluding that using smaller aggregate size can decrease the concrete compressive strength but increase ductility. In contrast, CSA S806 code (CSA, 2012) states that more lateral spirals are needed with a small aggregate size to compensate for the loss in strength capacity. This is impractical in designing hollow concrete columns with GFRP reinforcement. On the other hand, the columns with higher f'_c evidenced lower deformation capacity at failure, despite having the same reinforcement details. To illustrate, column B-100-44.0 had a ductility factor 14.1%, 31.2%, and 33.3% lower than columns B-100-36.8, B-100-26.8, and B-100-21.2, respectively (Table 4). This finding is related to the increased brittleness of concrete with higher f'_c (Cui and Sheikh, 2010, Hadhood, et al., 2016, Hadi, et al., 2017). As a result, the tested GFRP-reinforced HCCs with higher f'_c exhibited lower structural performance than those with lower f'_c but the same construction details.

Load-Strain Behavior

Figure 10 shows the load and axial strain (negative sign) in the longitudinal GFRP bars and lateral strain (positive sign) in the spirals for Group B columns. As shown, the axial strain measured in the longitudinal bars ascended linearly until P_{n1}. The maximum measured axial longitudinal bar strain at P_{n1} ($\varepsilon_{b,P_{n1}}$) was 3,308 $\mu\varepsilon$, 2,318 $\mu\varepsilon$, 2,151 $\mu\varepsilon$, and 2,181 $\mu\varepsilon$ in columns B-100-21.2, B-100-26.8, B-100-36.8, and B-100-44.0, respectively. This represents 10% to 16% of the ultimate tensile strain of the GFRP bars. Table 4 gives the ultimate recorded concrete strain ($\varepsilon_{c,P_{n1}}$) in columns B-100-26.8 and B-100-36.8 as 3,162 $\mu\varepsilon$ and 2,013 $\mu\varepsilon$, respectively, which is close to the recorded axial strain in the GFRP bars, while column H-100-44.0 recorded a strain of only 1,604 $\mu\varepsilon$, owing to early crack formation in the outer concrete cover. Moreover, the increase of f_c' reduced the spiral engagement at P_{n1} [Table 4], since Poisson's ratio decreases as f_c' increases, as also suggested by Simmons (1955). Generally, the strain readings ($\varepsilon_{s,P_{n1}}$) were less than 5% of the ultimate tensile strain of the GFRP spirals at P_{n1}.

After the concrete-cover spalling, GFRP bars and spirals experienced an increase in strain values, suggesting the outward deformation of the column and activation of reinforcement confining pressure on the concrete core. At failure, the maximum axial compressive strain measured in the longitudinal bars was 8,056 $\mu\varepsilon$, 10,692 $\mu\varepsilon$, 14,700 $\mu\varepsilon$, and 1,0940 $\mu\varepsilon$ (38.4%, 50.9%, 70%, and 52.1% of tensile strain) in columns B-100-21.2, B-100-26.8, B-100-36.8, and B-100-44.0, respectively, as can be seen in Fig. 10. Figure 10 also shows that the lateral strain in the spirals plateaued after P_{n1} in columns B-100-21.2, B-100-26.8, and B-100-36.8 until reaching of 3,052 $\mu\varepsilon$, 12,740 $\mu\varepsilon$, and 15,883 $\mu\varepsilon$. Although the spirals in column B-100-44.0 showed a strength enhancement, it was stopped early at 2,742 $\mu\varepsilon$ because of bar rupture. Moreover, the low spiral strain recorded by column B-100-21.2 is related to the specimen's failure mode, since the unconfined concrete part was gradually smashed without effective engagement from the lateral GFRP spirals.

Volumetric Strain Behavior

The tested HCCs exhibited an increase in volumetric strain with increasing f_c' [Fig. (11)]. Similar to Group A columns, a lateral strain factor of 3 gives a slope of (1-2*v*). In general, a negative volumetric strain was observed owing to the concrete cover spalling. An ascending slope was then observed due to the lateral expansion of the GFRP spirals, with the slope descending again when the concrete core failed. Interestingly, column B-100-44.0 showed no negative volumetric strain, which means high shortening axial strain with insignificant lateral expansion. This resulted in a volume reduction phenomenon due to the high energy stored in the concrete and longitudinal bars ended with a massive failure in those components owing to the lack in lateral reinforcement. In this case, more spirals are recommended to reinforce hollow concrete columns with high f_c', as indicated by CSA S806 code (CSA, 2012). This finding is supported by the low lateral strain in Fig. 10 owing to the low lateral expansion of the high compressive-strength concrete because of the Poisson's ratio effect, as suggested by Simmons (1955).

THEORETICAL PREDICTION

Design-Load Capacity

The first peak (P_{n1}) in the load–deformation curve (Figs. 4 and 9) was considered the maximum design capacity of the specimens. This peak represents the contribution of the gross concrete and the longitudinal GFRP bars in compression. It should be noted that current design standards ignore the contribution of GFRP bars (CSA, 2012, ACI, 2015) in compression members. The concrete contribution was calculated by multiplying f_c' and the cross-sectional area of the concrete (A_c), excluding the bar area. A reduction factor (α_2) of 0.85 for f_c' less than 50 MPa was applied, as suggested by ACI 318-8 code (ACI, 2008) and AS3600 code (AS3600, 2011), representing the difference between full-scale reinforced-concrete columns and concrete cylinders in terms of the strength, size, and shape. On the other hand, the GFRP bars' load contribution was calculated as the product of the axial strain in the longitudinal GFRP bars (ε_{FRP}) at P_{n1}, the elastic modulus of the GFRP bars (E_{FRP}), and the nominal cross-sectional area (A_{FRP}). It should mentioned that the axial load contribution of GFRP bars at P_{n1} varied from 6.9% to 25.2%, with the higher f_c' values leading to a significant reduction in this percentage. The experimental results show that the maximum recorded axial strain of longitudinal bars at P_{n1} was 0.003, so this value was used in predicting the design-load capacity (P_n), as shown in Eq. (2) and Table 5. Interestingly, this strain value is consistent with the ultimate concrete strain in compression recommended by ACI 318-14M (ACI, 2014). This strain value is also similar to the findings of Park and Paulay (1975) and Sheikh and Uzumeri (1980), who observed concrete-cover spalling at a strain between 0.003 and 0.004. For comparison, the load capacity of the HCCs neglecting the contribution of the GFRP bars was also calculated and compared with the experimental results (see Table 5).

$$P_n = \alpha_2 \times f_c' \times A_c + 0.003 \times E_{FRP} \times A_{FRP} \qquad \text{Eq. (2)}$$

Second Peak Load and Failure Point

Reinforcing the HCCs laterally with GFRP spirals resulted in the columns to exhibit post-loading behavior as a result of lateral confinement. The spirals laterally restricted the expansion of concrete core and limiting buckling of the longitudinal GFRP bars, allowing the columns to keep resisting applied loads until reaching P_{n2} and showing the maximum confined strength. The contribution of the GFRP spirals [Fig. 12(a)] was determined by evaluating the relationship between the confining stress (f_l) [Eq. (4)], as a function of the lateral confinement stiffness ratio (ρ_v) [Eq. (3)], and the effective concrete-core strength (f_{ce}) [Eq. (7 and 8) and Fig. (13)]. A confinement effectiveness factor (K_e) [Fig. 12(b)] was applied to account for the discontinuity in the lateral confining stress in the concrete core at the unconfined sections between spirals [Eq. (6)]. Equation (4) was adopted from Karim, et al. (2016), who evaluated the lateral confinement of the solid GFRP-reinforced columns, and Eq. (6) from Mander, et al. (1988) to reduce the lateral-stress effectiveness caused by the discontinuous lateral confinement. Both equations take into account the inner void. Ratio of the average recorded spiral strain ($\varepsilon_{s,P_{n2}}$) to the ultimate tensile strain of spirals (K_{ε}) in Eq. (4) equals to 0.39. The influence of the lateral-stiffness ratio (ρ_v) on the effective concrete strength (f_{ce}) was obtained and plotted in Fig. 13. The decreasing trend line represents the effect of ,spiral spacing [Eq. (7)], while the increasing trend line represents the effect of increasing concrete compressive strength [Eq. (8)]. These trends are valid for the test results of this study. The contribution of the GFRP bars at the second peak load ($\varepsilon_{b,P_{n2}}$) was measured experimentally corresponding to an average axial strain equal to 0.0095 (Table 3 and 4). This strain value was therefore taken as the maximum strain of the confined concrete core. This axial-strain value evidently is close to 0.010 and 0.008, as suggested by Zahn, et al. (1990) and Hoshikuma and Priestley (2000), respectively, for the maximum observed axial strain of the confined concrete in steel-reinforced hollow concrete columns. The theoretical second peak load (P_{n2t}) can then be calculated by adding the contribution of the confined concrete core and the GFRP bars at an axial strain (ε_{FRP2}) of 0.0095 [Eq. (9)]. It was observed that the GFRP bars contributed in a range of 40% to 69% from P_{n2} and was negatively affected by increasing f_c' values. The axial-load contribution of the GFRP bars at P_{n2} was calculated by multiplying $\varepsilon_{s,P_{n2}}$by A_{FRP} and E_{FRP} and then divided the result by the corresponding P_{n2}.

Table 6 shows the comparison between the theoretical and experimental results, which are in good agreement. Nevertheless, the P_{n2t} of column H-50-26.8 corresponds to 85% of the P_{n2} due to the lower predicted axial strain of the GFRP bars compared to the experimental one. Consequently, a more comprehensive study is required to investigate the compressive behavior of GFRP bars with different unbraced lengths. On the other hand, P_{n2t} of column H-100-21.2

corresponds to 118% of the P_{n2} due to the use of different size aggregate, which reduced the sample's overall strength.

$$\rho_v = \frac{k_e f_l}{f_c'} \tag{3}$$

$$f_l = \frac{2A_h K_\varepsilon f_{bent}}{S(D_s - D_i)} \tag{4}$$

$$f_{bent} = (0.05\frac{r}{d_b} + 0.3)f_u \leq f_u \text{ (CSA, 2012)} \tag{5}$$

$$k_e = \frac{A_{ce}}{A_{cc}} = \frac{\frac{\pi}{4}\left(\left(D_s - \frac{S'}{4}\right)^2 - D_i^2\right)}{\frac{\pi}{4}(D_s^2 - D_i^2)(1-\rho_e)} \tag{6}$$

$$f_{ce} = 4.4\ln(\rho_v) + 31.3 \tag{7}$$

$$f_{ce} = 0.57{\rho_v}^{-1.6} \tag{8}$$

$$P_{n2t} = f_{ce}A_{cc} + \varepsilon_{FRP2}A_{FRP}E_{FRP} \tag{9}$$

where D_s and D_i are the concrete core diameter and the void diameter, respectively. S and S' are the center-to-center distance and the clear spacing between spirals, respectively. A_{ce} is the concrete core area with the damage effect, whereas, A_{cc} is the concrete core area excluding the longitudinal bars area.

CONCLUSIONS

This study investigated the effect of using various lateral spiral spacing and the effect of concrete compressive strength on the behavior of concentrically loaded hollow concrete columns reinforced with GFRP bars. Moreover, the applicability of the existing equations for determining the design-load capacity of GFRP-reinforced concrete members in compression was validated, and a model was proposed to describe the post-loading behavior of the columns. Based on the results of this study, the following conclusions can be drawn.

- The GFRP-reinforced hollow concrete columns with closer lateral spiral spacing exhibited higher axial-load capacity than those with broader spacing owing to the early activation of confinement. Decreasing the spacing from 150 mm to 50 mm increased the capacity by 8%. Moreover, narrowing the spiral spacing led to more progressive failure of the concrete core and longitudinal bars.

- Reducing the spiral spacing from 150 mm and 100 mm to 50 mm increased the ductility and confined strength of the columns by 98% and 69%, respectively. This outcome was due to the increased axial-strain capacity of the longitudinal bars with reduced unbraced length and less extent of the unconfined concrete core between spirals.
- Using concrete with higher compressive strength increased the axial-load capacity and stiffness of the columns by up to 107% and 70%, respectively, due to the concrete higher elastic modulus. Column failure, however, changed from ductile to brittle.
- The columns made with concrete with higher compressive strength had lower confinement efficiency and ductility compared to the columns with lower compressive strength. Increasing the concrete compressive strength from 21.6 MPa to 44.0 MPa decreased the confinement efficiency and ductility by 7% and 50%, respectively, due to the higher brittleness of concrete with higher compressive strength.
- The design-load capacity of GFRP-reinforced hollow concrete columns can be reliably predicted by considering the contribution of the concrete gross section and the longitudinal GFRP bars at 0.003 axial strain. Herein, the contribution of the longitudinal GFRP bars to load capacity ranged from 10% to 20%.
- The second peak-load capacity of hollow concrete columns reinforced with GFRP bars can be described well by considering the contribution of the longitudinal GFRP bars at an ultimate axial strain of 0.0095 and the effective area of the confined concrete core.

ACKNOWLEDGEMENTS

The authors are grateful to Pultrall Canada and Inconmat V-ROD Australia for providing the GFRP bars and spirals. The assistance of the postgraduate students and technical staff at the Centre of Future Materials (CFM) is also acknowledged. The first author is also grateful for the doctoral scholarship provided by Tafila Technical University (TTU) in Jordan.

REFERENCES

ACI (2008). "Building Code Requirements for Structural Concrete (ACI 318-08) and Commentary." *ACI Committee 318, American Concrete Institute, Farmington Hills, MI*, 471.

ACI (2014). "(American Concrete Institute), Building code requirements for structural concrete." *ACI 318-14M, Farmington Hills, MI*.

ACI (2015). "Guide for the Design and Construction of Concrete Reinforcedwith FRP Bars (440.1R-15)." *American Concrete Institute, Farmington Hills, MI*.

AlAjarmeh, O. S., Manalo, A., Benmokrane, B., Karunasena, W., Mendis, P., and Nguyen, K. (2019a). "Compressive behavior of axially loaded circular hollow concrete columns reinforced with GFRP bars and spirals." *Construction and Building Materials*, 194, 12-23.

AlAjarmeh, O. S., Manalo, A. C., Benmokrane, B., Karunasena, W., and Mendis, P. (2019b). "Axial performance of hollow concrete columns reinforced with GFRP composite bars with different reinforcement ratios." *Composite Structures*, 213(1), 12.

AS3600 (2011). *Reinforced Concrete Design : in accordance with AS 3600-2009*, Cement & Concrete Aggregates Australia : Standards Australia, Sydney, N.S.W.

ASTM (2011b). "Standard test method for tensile properties of fiber reinforced polymer matrix composite bars." *ASTM D7205/D7205M-06, West Conshohocken, PA*.

ASTM C31 (2015). "Standard Practice for Making and Curing Concrete Test Specimens in the Field." *ASTM International, West Conshohocken, PA*.

ASTM C39 (2015). "Standard Test Method for Compressive Strength of Cylindrical Concrete Specimens." *ASTM International, West Conshohocken, PA.*

Benmokrane, B., Chaallal, O., and Masmoudi, R. (1995). "Glass fibre reinforced plastic (GFRP) rebars for concrete structures." *Construction and Building Materials*, 9(6), 353-364.

Benmokrane, B., Manalo, A., Bouhet, J.-C., Mohamed, K., and Robert, M. (2017). "Effects of Diameter on the Durability of Glass Fiber–Reinforced Polymer Bars Conditioned in Alkaline Solution." *Journal of Composites for Construction*, 21(5), 04017040.

Cascardi, A., Micelli, F., and Aiello, M. A. (2016). "Unified model for hollow columns externally confined by FRP." *Engineering Structures*, 111, 119-130.

Cassidy, M., Waldie, J., and Palanisamy, S. (2015). "A Method to Estimate the Cost of Corrosion for Australian Defence Force Aircraft."

CSA (2012). *Design and construction of building structures with fibre-reinforced polymers*, Canadian Standards Association, CAN/CSA-S806-12, Rexdale, ON, Canada.

Cui, C., and Sheikh, S. (2010). "Experimental Study of Normal-and High-Strength Concrete Confined with Fiber-Reinforced Polymers." *Journal of Composites for Construction*, 14(5).

Fillmore, B., and Sadeghian, P. (2018). "Contribution of Longitudinal GFRP Bars in Concrete Cylinders under Axial Compression." *Canadian Journal of Civil Engineering*, 45(6), 458-468.

Hadhood, A., Mohamed, H. M., and Benmokrane, B. (2016). "Experimental Study of Circular High-Strength Concrete Columns Reinforced with GFRP Bars and Spirals under Concentric and Eccentric Loading." *Journal of Composites for Construction*, 04016078.

Hadi, M., and Le, T. (2014). "Behaviour of hollow core square reinforced concrete columns wrapped with CFRP with different fibre orientations." *Construction and Building Materials*, 50, 62-73.

Hadi, M. N., Hasan, H. A., and Sheikh, M. N. (2017). "Experimental Investigation of Circular High-Strength Concrete Columns Reinforced with Glass Fiber-Reinforced Polymer Bars and Helices under Different Loading Conditions." *Journal of Composites for Construction*, 04017005.

Hadi, M. N., Karim, H., and Sheikh, M. N. (2016). "Experimental investigations on circular concrete columns reinforced with GFRP bars and helices under different loading conditions." *Journal of Composites for Construction*, 20(4).

Hoshikuma, J.-i., and Priestley, M. (2000). "Flexural behavior of circular hollow columns with a single layer of reinforcement under seismic loading." *SSRP*, 13.

Karim, H., Sheikh, M. N., and Hadi, M. N. (2016). "Axial load-axial deformation behaviour of circular concrete columns reinforced with GFRP bars and helices." *Construction and Building Materials*, 112, 1147-1157.

Kusumawardaningsih, Y., and Hadi, M. N. (2010). "Comparative behaviour of hollow columns confined with FRP composites." *Composite Structures*, 93(1), 198-205.

Lee, J.-H., Choi, J.-H., Hwang, D.-K., and Kwahk, I.-J. (2015). "Seismic performance of circular hollow RC bridge columns." *KSCE Journal of Civil Engineering*, 19(5), 1456-1467.

Liang, X., Beck, R., and Sritharan, S. (2015). "Understanding the Confined Concrete Behavior on the Response of Hollow Bridge Columns."

Lignola, G. P., Nardone, F., Prota, A., De Luca, A., and Nanni, A. (2011). "Analysis of RC Hollow Columns Strengthened with GFRP." *Journal of Composites for Construction*, 15(4), 545-556.

Lignola, G. P., Prota, A., Manfredi, G., and Cosenza, E. (2007). "Experimental performance of RC hollow columns confined with CFRP." *Journal of Composites for Construction*, 11(1), 42-49.

Lignola, G. P., Prota, A., Manfredi, G., and Cosenza, E. (2008). "Unified theory for confinement of RC solid and hollow circular columns." *Composites Part B: Engineering*, 39(7), 1151-1160.

Manalo, A., Aravinthan, T., Mutsuyoshi, H., and Matsui, T. (2012). "Composite behaviour of a hybrid FRP bridge girder and concrete deck" *Advances in Structural Engineering*, 15(4), 589-600.

Manalo, A., Benmokrane, B., Park, K.-T., and Lutze, D. (2014). "Recent developments on FRP bars as internal reinforcement in concrete structures." *Concrete in Australia*, 40(2), 46-56.

Mander, J. B., Priestley, M. J., and Park, R. (1988). "Theoretical stress-strain model for confined concrete." *Journal of structural engineering*, 114(8), 1804-1826.

Maranan, G., Manalo, A., Benmokrane, B., Karunasena, W., and Mendis, P. (2016). "Behavior of concentrically loaded geopolymer-concrete circular columns reinforced longitudinally and transversely with GFRP bars." *Engineering Structures*, 117, 422-436.

Maranan, G., Manalo, A., Benmokrane, B., Karunasena, W., Mendis, P., and Nguyen, T.Q. (2018). " Shear behaviour of geopolymer-concrete beams transversely reinforced with continuous rectangular GFRP composite spirals." *Composite Structures*, 187, 454-465.

Mirmiran, A., and Shahawy, M. (1997). "Behavior of concrete columns confined by fiber composites." *Journal of structural engineering*, 123(5), 583-590.

Mo, Y., Wong, D., and Maekawa, K. (2003). "Seismic performance of hollow bridge columns." *Structural Journal*, 100(3), 337-348.

Mohamed, H. M., Afifi, M. Z., and Benmokrane, B. (2014). "Performance evaluation of concrete columns reinforced longitudinally with FRP bars and confined with FRP hoops and spirals under axial load." *Journal of Bridge Engineering*, 19(7), 04014020.

Morales, S. M. (1982). "Spirally-reinforced high-strength concrete columns." *NASA STI/Recon Technical Report N*, 84.

Neville, A. M. (1995). *Properties of concrete*, Longman London.

Pantelides, C. P., Gibbons, M. E., and Reaveley, L. D. (2013). "Axial load behavior of concrete columns confined with GFRP spirals." *Journal of Composites for Construction*, 17(3), 305-313.

Park, R., and Paulay, T. (1975). *Reinforced concrete structures*, John Wiley & Sons.

Saatcioglu, M., and Razvi, S. R. (1992). "Strength and ductility of confined concrete." *Journal of Structural engineering*, 118(6), 1590-1607.

Sheikh, S. A., and Uzumeri, S. M. (1980). "Strength and ductility of tied concrete columns." *Journal of the structural division*, 106(ASCE 15388 Proceeding).

Simmons, J. (1955). "Poisson's ratio of concrete: a comparison of dynamic and static measurements." *Magazine of Concrete Research*, 7(20), 61-68.

Tannous, F. E. (1997). "Durability of non-metallic reinforcing bars and prestressing tendons."

Tobbi, H., Farghaly, A. S., and Benmokrane, B. (2014). "Behavior of concentrically loaded fiber-reinforced polymer reinforced concrete columns with varying reinforcement types and ratios." *ACI Structural Journal*, 111(2), 375.

Verma, S. K., Bhadauria, S. S., and Akhtar, S. (2014). "Monitoring corrosion of steel bars in reinforced concrete structures." *The scientific world journal*, 2014.

Zahn, F., Park, R., and Priestley, M. (1990). "Flexural strength and ductility of circular hollow reinforced concrete columns without confinement on inside face." *Structural Journal*, 87(2), 156-166.

FOOTNOTES

This manuscript includes the following symbols:

$\alpha_2 =$ Effect of the concrete compressive strength factor (0.85)

$A_g =$ Total cross-section area (mm^2)

$A_{core} =$ Effective core area denoted by the distance between spiral centres (mm^2)

$A_c =$ Concrete area in the section (without the area of GFRP bars) ($A_g - A_{FRP}$) (mm^2)

$A_{cc} =$ Concrete core area (without the area of GFRP bars) ($A_{core} - A_{FRP}$) (mm^2)

$A_{ce} =$ Area of the concrete core excluding the crushed concrete part due to unconfined concrete between the spirals (mm^2)

$A_{FRP} =$ Total area of the GFRP bars (mm^2)

$A_h =$ GFRP-spiral cross-sectional area (mm^2)

$C.E. =$ Confinement efficiency

$\Delta_y =$ Yield deformation (mm)

$\Delta_u =$ Ultimate deformation (mm)

$D.F. =$ Ductility factor

$d_b =$ Bar diameter of lateral reinforcement (mm)

$D_i =$ Diameter of the inner void (mm)

$D_s =$ Diameter of spirals on-centres (mm)

$\varepsilon_{b,P_{n1}} =$ Axial strain of GFRP bars at P_{n1}

$\varepsilon_{b,P_{n2}} =$ Axial strain of GFRP bars at P_{n2}

$\varepsilon_{c,P_{n1}} =$ Maximum recorded concrete strain at P_{n1}

$\varepsilon_{co} =$ Unconfined concrete strain

$\varepsilon_{FRP2} =$ Maximum strain of the GFRP bars at P_{n2}

$\varepsilon_{s,P_{n1}} =$ Axial strain of GFRP spirals at P_{n1}

$\varepsilon_{s,P_{n2}} =$ Axial strain of GFRP spirals at P_{n2}

$\varepsilon_u =$ Ultimate tensile strain

$E_{FRP} =$ Elastic modulus of GFRP bars (MPa)

$f_{bent} =$ Tensile strength of bent GFRP bars, ACI 400.1R-15 (ACI, 2015) (MPa) (Eq. 5)

$f_c' =$ Concrete compressive strength at the day of testing the HCCs (MPa)

$f_{cc}' =$ Confined strength of the concrete core after concrete-cover spalling (MPa)

$f_{co} =$ Unconfined concrete strength ($0.85 f_c'$) (MPa)

$f_{ce} =$ Effective concrete strength (MPa) (Eqns. 7 and 8)

$f_l =$ Lateral confining stress (MPa) (Eq. 4)

$f_u =$ Ultimate tensile strength of GFRP reinforcements (MPa)

$k_e =$ Reduction factor regarding the vertical unconfined area between spirals (Eq. 6)

$K_\varepsilon =$ The proportion of ultimate strain in GFRP spirals before failure to their ultimate tensile strength (0.39 as an average)

$P_{n1} =$ First axial peak load (kN)

$P_n =$ Theoretical design load capacity (kN)

$P_{n2} =$ Experimental second axial peak load (kN)

$P_{nt2} =$ Theoretical second axial peak load (kN)

$P_f =$ Failure load (kN)

$\rho =$ Reinforcement ratio with respect to the total cross-section area (A_g)

$\rho_e =$ Effective reinforcement ratio with respect to the effective core area

$\rho_v =$ lateral stiffness ratio (Eq. 3)

$r =$ Inner radius of the spiral (mm)

$S =$ Vertical spacing of spirals on-centres (mm)

$S' =$ Clear vertical spacing between spirals (mm)

List of Figures:

List of Tables:

Tables

Table 1. Properties for the GFRP reinforcement (Benmokrane, et al., 2017)

Property		Test Method	Sample	No. 5	No. 3
Physical	Nominal bar diameter, mm	CSA S806, Annex A (CSA, 2012)	9	15.9	9.5
	Nominal bar area, mm^2	CSA-S806, Annex A (CSA, 2012)	9	198.5	70.8
	Actual bar's cross-sectional area by immersion test, mm^2			224.4 (1.2)	83.8 (1.9)
Mechanical	Ultimate tensile strength, f_u(MPa)	ASTM D7205/D7205M-06 (ASTM, 2011b)	6	1237 (33.3)	1315 (31.1)
	Modulus of elasticity, E_{FRP} (GPa)	ASTM D7205/D7205M-06 (ASTM, 2011b)	6	60.0 (1.3)	62.5 (0.4)
	Ultimate strain, ε_u(%)	ASTM D7205/D7205M-06 (ASTM, 2011b)	6	2.1 (0.1)	2.3 (0.1)

Table 2. Concrete-column matrices and details

Specimens	Volumetric Ratio (%)	Spacing (mm)	Concrete Compressive Strength (MPa)
A-N/A-26.8	0.00	N/A	26.8
A-150-26.8	1.28	150	26.8
A&B-100-26.8	1.93	100	26.8
A-50-26.8	3.84	50	26.8
B-100-21.2	1.93	100	21.2
B-100-36.8	1.93	100	36.8
B-100-44.0	1.93	100	44.0

Table 3. Test results of group A columns

Sample	**Stiffness** kN/mm	P_{n1} kN	**Yield deformation,** Δ_y mm	P_{n2} kN	**Ultimate deformation,** Δ_u mm	P_f kN	***D.F.***	f'_{cc} MPa	***C.E.***	$\varepsilon_{c,P_{n1}}$ $\mu\varepsilon$	$\varepsilon_{b,P_{n1}}$ $\mu\varepsilon$	$\varepsilon_{b,P_{n2}}$ $\mu\varepsilon$	$\varepsilon_{s,P_{n1}}$ $\mu\varepsilon$	$\varepsilon_{s,P_{n2}}$ $\mu\varepsilon$
A-N/A-26.8	177	1,022	7.3	-	-	-	-	-	-	1,455	1,645	-	-	-
A-150-26.8	163	1,108	8.3	1,110	16.1	1,083	1.94	50.5	2.20	1,952	3,902	10,070	2,435	4,478
A-100-26.8	132	1,189	9.3	1,102	23.3	1,015	2.53	50.1	2.19	2,162	2,318	8,951	1,104	8,850
A-50-26.8	120	1,197	11.4	1,434	43.9	1,002	3.85	65.2	3.07	2,524	3,884	12,850	2,514	6,318

Table 4. Test results of group B columns

Sample	**Stiffness kN/mm**	P_{n1} **kN**	Δ_y **mm**	P_{n2} **kN**	Δ_u **mm**	P_f **kN**	***D.F.***	f'_{cc} **MPa**	***C.E.***	$\varepsilon_{c,P_{n1}}$ $\mu\varepsilon$	$\varepsilon_{b,P_{n1}}$ $\mu\varepsilon$	$\varepsilon_{b,P_{n2}}$ $\mu\varepsilon$	$\varepsilon_{s,P_{n1}}$ $\mu\varepsilon$	$\varepsilon_{s,P_{n2}}$ $\mu\varepsilon$
B-100-21.2	121	907	8.0	849	21.1	642	2.64	38.6	2.14	-	3,308	7,554	1,203	3,052
B-100-26.8	132	1,189	9.3	1,102	23.3	1,073	2.53	50.1	2.19	2,162	2,318	8,951	1,104	8,850
B-100-36.8	169	1,570	9.5	1,424	19.5	1,309	2.05	64.7	2.07	2,013	2,151	9,509	823	11,856
B-100-44.0	196	1,880	9.6	1,644	16.9	1,481	1.76	74.8	2.00	1,604	2,181	9,143	361	2,673

Table 5. Comparison between experimental and theoretical axial-load capacity values

Column	Experimental Load Capacity (kN)	Theoretical Load (CSA, 2012, ACI, 2015) (kN) (Error %)	Theoretical Load in Proposed Model (kN) (Error %)
A-N/A-26.8	1,022	973 (5%)	1,160 (-12%)
A-150-26.8	1,108	973 (12%)	1,160 (-5%)
A/B-100-26.8	1,189	973 (18%)	1,160 (2%)
A-50-26.8	1,197	973 (19%)	1,160 (3%)
B-100-21.2	907	770 (15%)	962 (-6%)
B-100-36.8	1,570	1,336 (15%)	1,513 (3%)
B-100-44.0	1,880	1,597 (15%)	1,767 (6%)
Average error	-	14%	2%

Table 6. Comparison between the theoretical and experimental second peak load

Column	k_e	f_l (MPa)	ρ_v	f_{ce} (MPa)	P_{n2t} (kN)	P_{n2t} / P_{n2}
A-150-26.8	0.60	3.7	0.084	19.4	1,082	0.97
A&B-100-26.8	0.75	5.6	0.157	21.4	1,124	1.01
A-50-26.8	0.92	11.2	0.383	25.2	1,203	0.85
B-100-21.2	0.75	5.6	0.199	15.4	999	1.18
B-100-36.8	0.75	5.6	0.115	36.6	1440	1.01
B-100-44.0	0.75	5.6	0.096	48.7	1691	1.03

(a) Longitudinal GFRP bars

(b) GFRP spirals

Fig. 1. GFRP reinforcement

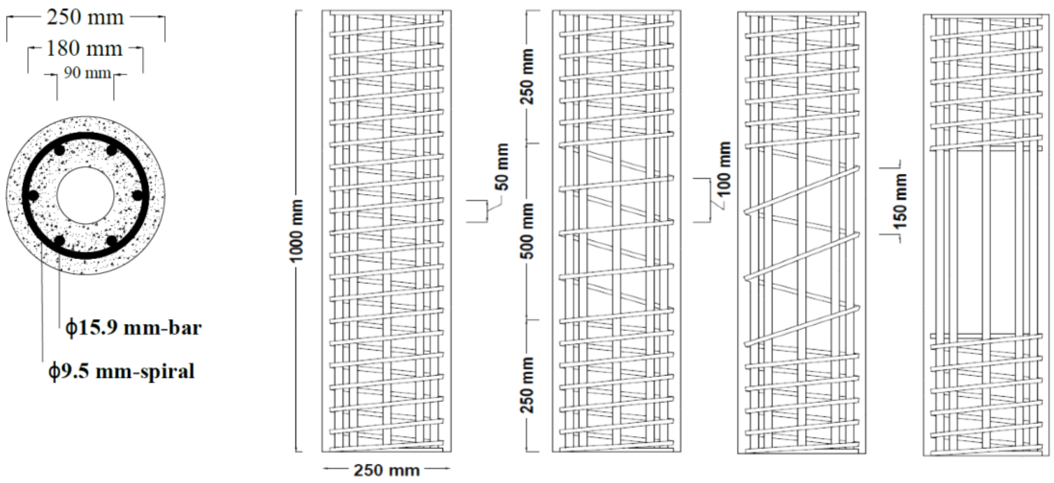

A-50-26.8

A&B-100-(21.2, 26.8, 36.8, and 44.0)

A-150-26.8

A-N/A-26.8

Fig. 2. Typical cross section of columns and lateral spiral details

Figure 03 Click here to access/download;Figure;Fig. 3.pdf

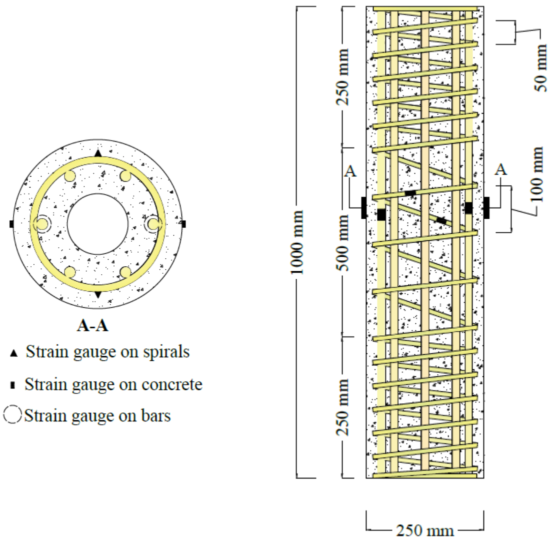

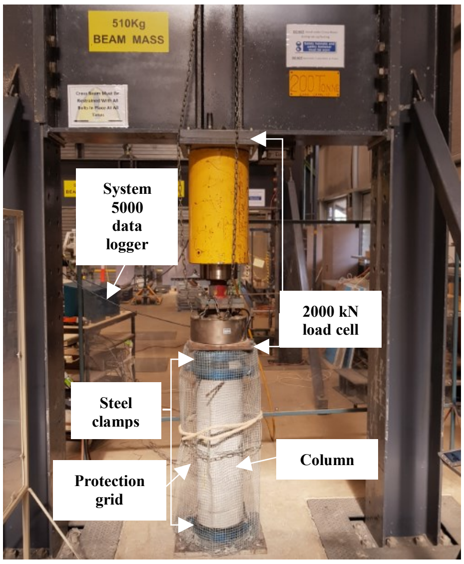

(a) Location of strain gauges

(b) Test setup

Fig. 3. Test setup and instrumentation for the hollow concrete columns

(a) A-N/A-26.8 **(b) A-150-26.8** **(c) A-100-26.8** **(d) A-50-26.8**

Fig. 4. The final failure of the columns in Group A

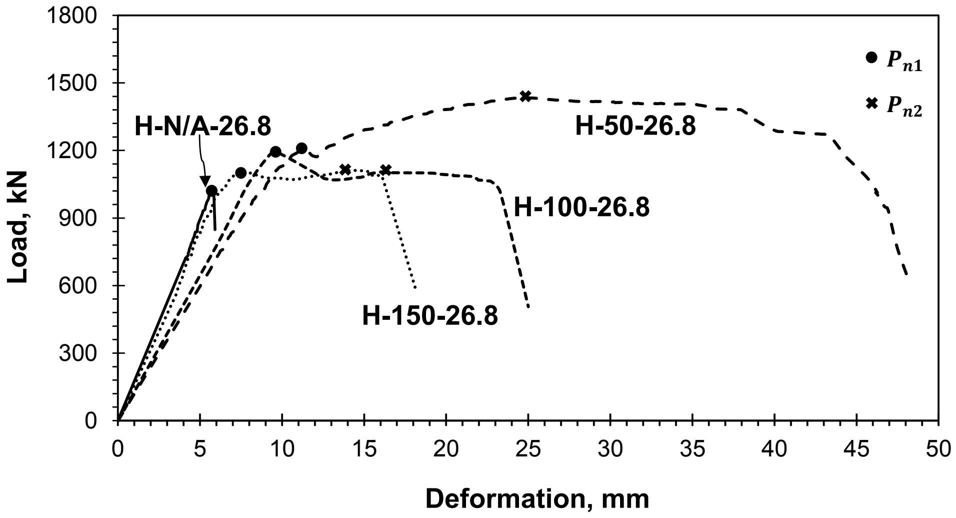

Fig. 5. Load–deformation behavior of group A columns

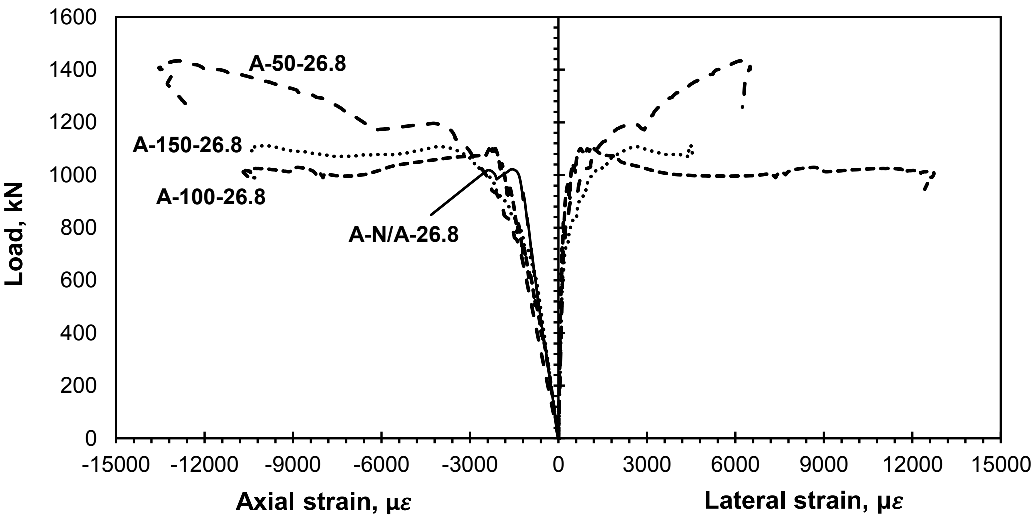

Fig. 6. Axial and lateral strain versus applied load for Group A columns

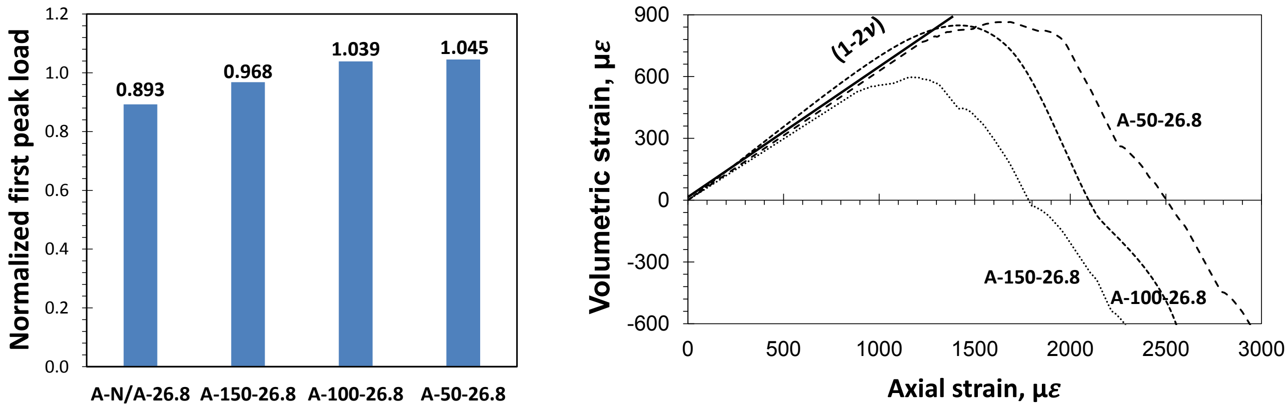

(a) First peak-load enhancement (b) Volumetric-strain versus axial-strain behavior

Fig. 7. Strength enhancement and volumetric-strain behavior of Group A columns

(a) B-100-21.2 **(b) B-100-26.8** **(b) B-100-36.8** **(c) B-100-44.0**

Fig. 8. The final failure of Group B columns

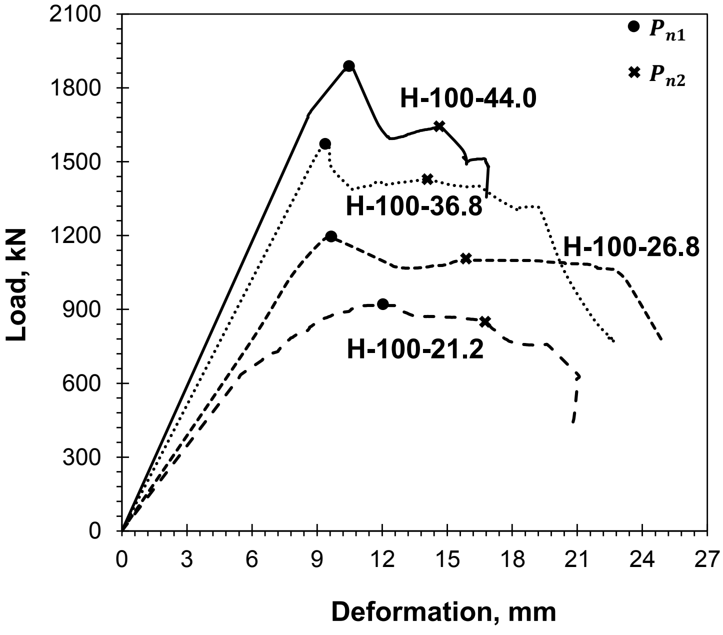

Fig. 9. Load–deformation behavior of group B columns

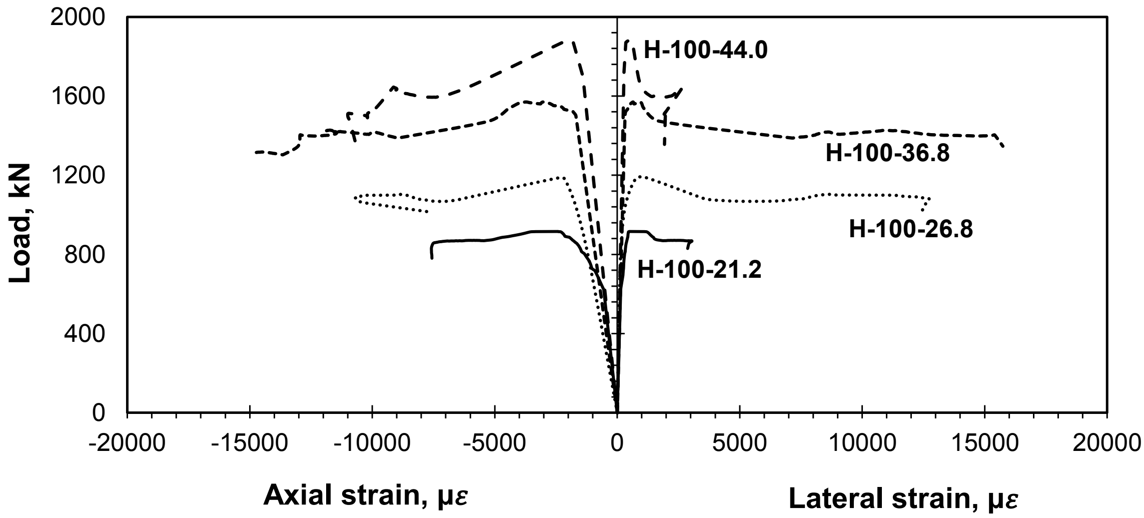

Fig. 10. Axial and lateral strain versus applied load for Group B columns

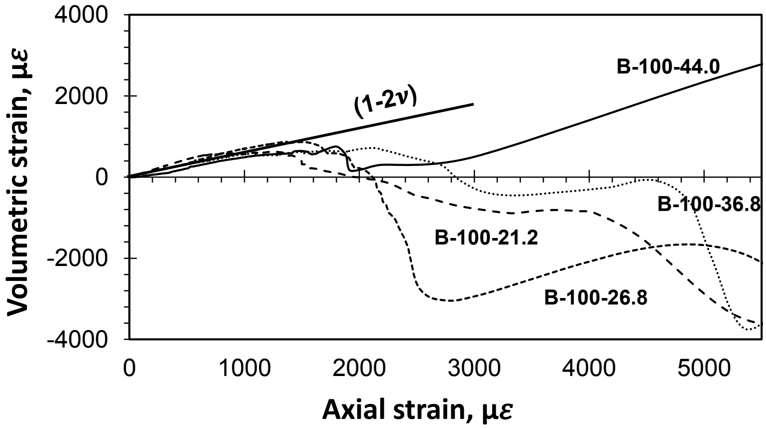

Fig. 11. Volumetric strain versus axial strain for Group B columns

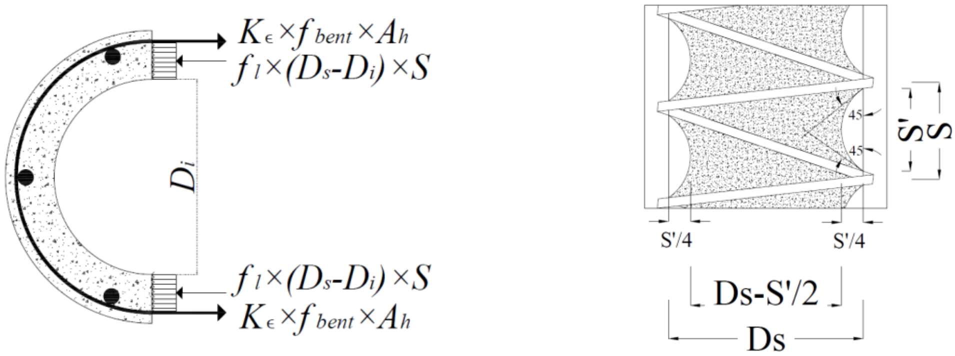

(a) Lateral confinement **(b)** Confinement effectiveness factor

Fig. 12. Lateral-confinement mechanism and confinement effectiveness factor

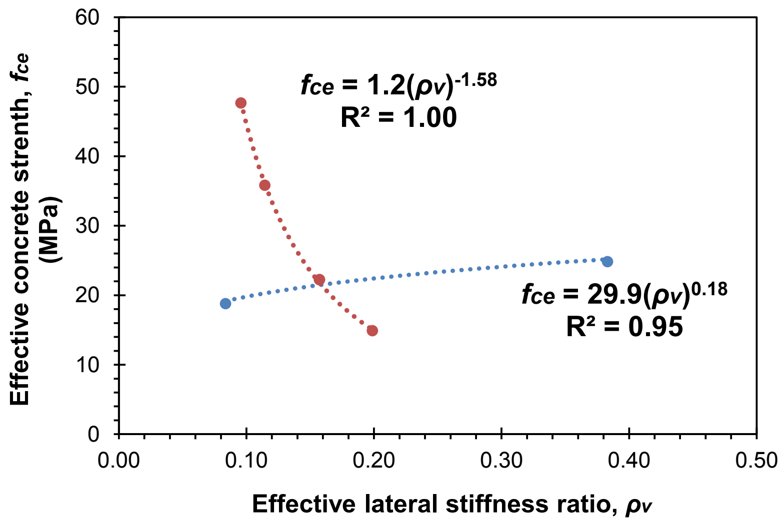

Fig. 13. Influence of lateral stiffness ratio (ρ_v) on the effective concrete strength (f_{ce})

ASCE Authorship, Originality, and Copyright Transfer Agreement

Publication Title: Journal of Composites for Construction

Manuscript Title: Effect of spiral spacing and concrete strength on behavior of GFRP-reinforced hollow concrete columns

Author(s) – **Names, postal addresses, and e-mail addresses of all authors**

Omar Alajarmeh, University of Southern Qld, Toowoomba, Qld 4350, Australia - omar.alajarmeh@usq.edu.au
Allan Manalo, Univ. of Southern Qld, Toowoomba, Qld 4350, Australia - manalo@usq.edu.au
Brahim Benmokrane, Univ. of Sherbrooke, Sherbrooke, Quebec, Canada - Brahim.Benmokrane@USherbrooke.ca
Warna Karunasena, Univ. of Southern Qld, Toowoomba, Qld 4350, Australia - karu.karunasena@usq.edu.au
Priyan Mendis, Univ of Melbourne, Victoria 3010, Australia - pamendis@unimelb.edu.au

I. Authorship Responsibility

To protect the integrity of authorship, only people who have significantly contributed to the research or project and manuscript preparation shall be listed as coauthors. The corresponding author attests to the fact that anyone named as a coauthor has seen the final version of the manuscript and has agreed to its submission for publication. Deceased persons who meet the criteria for coauthorship shall be included, with a footnote reporting date of death. No fictitious name shall be given as an author or coauthor. An author who submits a manuscript for publication accepts responsibility for having properly included all, and only, qualified coauthors.

I, the corresponding author, confirm that the authors listed on the manuscript are aware of their authorship status and qualify to be authors on the manuscript according to the guidelines above.

ALLAN MANALO	[signature]	28/02/2019
Print Name	Signature	Date

II. Originality of Content

ASCE respects the copyright ownership of other publishers. ASCE requires authors to obtain permission from the copyright holder to reproduce any material that (1) they did not create themselves and/or (2) has been previously published, to include the authors' own work for which copyright was transferred to an entity other than ASCE. Each author has a responsibility to identify materials that require permission by including a citation in the figure or table caption or in extracted text. Materials re-used from an open access repository or in the public domain must still include a citation and URL, if applicable. At the time of submission, authors must provide verification that the copyright owner will permit re-use by a commercial publisher in print and electronic forms with worldwide distribution. For Conference Proceeding manuscripts submitted through the ASCE online submission system, authors are asked to verify that they have permission to re-use content where applicable. Written permissions are not required at submission but must be provided to ASCE if requested. Regardless of acceptance, no manuscript or part of a manuscript will be published by ASCE without proper verification of all necessary permissions to re-use. ASCE accepts no responsibility for verifying permissions provided by the author. Any breach of copyright will result in retraction of the published manuscript.

I, the corresponding author, confirm that all of the content, figures (drawings, charts, photographs, etc.), and tables in the submitted work are either original work created by the authors listed on the manuscript or work for which permission to re-use has been obtained from the creator. For any figures, tables, or text blocks exceeding 100 words from a journal article or 500 words from a book, written permission from the copyright holder has been obtained and supplied with the submission.

ALLAN MANALO	[signature]	28/02/2019
Print name	Signature	Date

III. Copyright Transfer

ASCE requires that authors or their agents assign copyright to ASCE for all original content published by ASCE. The author(s) warrant(s) that the above-cited manuscript is the original work of the author(s) and has never been published in its present form.

The undersigned, with the consent of all authors, hereby transfers, to the extent that there is copyright to be transferred, the exclusive copyright interest in the above-cited manuscript (subsequently called the "work") in this and all subsequent editions of the work (to include closures and errata), and in derivatives, translations, or ancillaries, in English and in foreign translations, in all formats and media of expression now known or later developed, including electronic, to the American Society of Civil Engineers subject to the following:

- The undersigned author and all coauthors retain the right to revise, adapt, prepare derivative works, present orally, or distribute the work, provided that all such use is for the personal noncommercial benefit of the author(s) and is consistent with any prior contractual agreement between the undersigned and/or coauthors and their employer(s).
- No proprietary right other than copyright is claimed by ASCE.
- If the manuscript is not accepted for publication by ASCE or is withdrawn by the author prior to publication (online or in print), this transfer will be null and void.
- Authors may post a PDF of the ASCE-published version of their work on their employers' ***Intranet*** with password protection. The following statement must appear with the work: "This material may be downloaded for personal use only. Any other use requires prior permission of the American Society of Civil Engineers."
- Authors may post the ***final draft*** of their work on open, unrestricted Internet sites or deposit it in an institutional repository when the draft contains a link to the published version at www.ascelibrary.org. "Final draft" means the version submitted to ASCE after peer review and prior to copyediting or other ASCE production activities; it does not .include the copyedited version, the page proof, a PDF, or full-text HTML of the published version.

Exceptions to the Copyright Transfer policy exist in the following circumstances. Check the appropriate box below to indicate whether you are claiming an exception:

☐ **U.S. GOVERNMENT EMPLOYEES:** Work prepared by U.S. Government employees in their official capacities is not subject to copyright in the United States. Such authors must place their work in the public domain, meaning that it can be freely copied, republished, or redistributed. In order for the work to be placed in the public domain, ALL AUTHORS must be official U.S. Government employees. If at least one author is not a U.S. Government employee, copyright must be transferred to ASCE by that author.

☐ **CROWN GOVERNMENT COPYRIGHT:** Whereby a work is prepared by officers of the Crown Government in their official capacities, the Crown Government reserves its own copyright under national law. If ALL AUTHORS on the manuscript are Crown Government employees, copyright cannot be transferred to ASCE; however, ASCE is given the following nonexclusive rights: (1) to use, print, and/or publish in any language and any format, print and electronic, the above-mentioned work or any part thereof, provided that the name of the author and the Crown Government affiliation is clearly indicated; (2) to grant the same rights to others to print or publish the work; and (3) to collect royalty fees. ALL AUTHORS must be official Crown Government employees in order to claim this exemption in its entirety. If at least one author is not a Crown Government employee, copyright must be transferred to ASCE by that author.

☐ **WORK-FOR-HIRE:** Privately employed authors who have prepared works in their official capacity as employees must also transfer copyright to ASCE; however, their employer retains the rights to revise, adapt, prepare derivative works, publish, reprint, reproduce, and distribute the work provided that such use is for the promotion of its business enterprise and does not imply the endorsement of ASCE. In this instance, an authorized agent from the authors' employer must sign the form below.

☐ **U.S. GOVERNMENT CONTRACTORS:** Work prepared by authors under a contract for the U.S. Government (e.g., U.S. Government labs) may or may not be subject to copyright transfer. Authors must refer to their contractor agreement. For works that qualify as U.S. Government works by a contractor, ASCE acknowledges that the U.S. Government retains a nonexclusive, paid-up, irrevocable, worldwide license to publish or reproduce this work for U.S. Government purposes only. This policy DOES NOT apply to work created with U.S. Government grants.

I, the corresponding author, acting with consent of all authors listed on the manuscript, hereby transfer copyright or claim exemption to transfer copyright of the work as indicated above to the American Society of Civil Engineers.

ALLAN MANALO

Print Name of Author or Agent

Signature of Author of Agent 28/02/2019

Date

More information regarding the policies of ASCE can be found at http://www.asce.org/authorsandeditors

RESPONSE TO REVIEWERS' COMMENTS

Manuscript Ref. No.: CCENG-2684

Title of MS: "THE EFFECT OF SPIRAL SPACING AND CONCRETE COMPRESSIVE STRENGTH ON THE BEHAVIOR OF GFRP-REINFORCED HOLLOW CONCRETE COLUMNS"

Authors: Omar S. AlAjarmeh, Allan C. Manalo, Brahim Benmokrane, Warna Karunasena, Priyan Mendis.

Editor's Comments

This manuscript is to be revised. This revision should aim at addressing the technical and editorial critiques offered in the attached three peer reviews and the associate editor's summary.

Authors' Responses

The authors would like to thank the Editor for his efforts and time in reviewing the paper. The comments will surely enhance and add to the paper. In the following table, the authors have attempted to respect and answer the editor's comments.

No.	Editor's comments	Authors' responses
1	Title: for brevity, revise as "EFFECT OF SPIRAL SPACING AND CONCRETE STRENGTH ON BEHAVIOR OF GFRP-REINFORCED HOLLOW CONCRETE COLUMNS".	*This suggestion was implemented in **Lines 1-2**.*
2	L46-47: when a list of references is presented, the order should be chronological. The rest of the manuscript must be checked accordingly as the same issue appears elsewhere (for example, L49-50).	*This correction was implemented in **lines 45-46** and **49-50**. The whole manuscript was also checked and corrected for any errors in citing references.*
3	L129 and elsewhere in the manuscript: "ASTM C31" instead of	*This correction was implemented in **lines 138-140.***

	"ASTM/C31". Use a blank space instead of / after "ASTM".	
4	L599: insert "outcome" after "This".	*This correction was implemented in **line 619.***
5	L603: "concrete" instead of "concrete's".	*This correction was implemented in **line 623.***
6	Eliminate the gridlines from all plots (this request would be made during manuscript production anyways).	*This suggestion was implemented in all figures in the manuscript.*
7	L120: "Four compressive strengths of normal-strength concrete were used to cast the column samples"; here the meaning is that the strength casts the column sample. The syntax needs to be fixed. The same applies to numerous other parts of the manuscript.	*This correction was implemented in **line 129.** The manuscript has been proofread.*

Associate Editor's Comments

The associate editor's recommendation is to revise the manuscript as a technical paper. The topic is suitable for the Journal's audience. The attached three peer reviews offer a number of constructive technical and editorial comments. The authors should consider all these comments as they revise the manuscript.

Authors' Responses

The authors would like to thank the Editor for his efforts and time in reviewing the paper. The comments will surely enhance and add to the paper. In the following table, the authors have attempted to respect and answer the associate editor's comments.

No.	Editor's comments	Authors' responses
1	Provide your responses to the reviewer comments in your revision including strengthening the introduction section highlighting the difference in behavior between solid and hollow columns that initiated this research.	*This suggestion was implemented. The difference in the behavior between solid and hollow columns was brought out to highlight the benefits of hollow columns (**lines 93-102**).*

2	L43: "utility poles" instead of "electric poles".	*This suggestion was implemented in* ***line 42.***
3	L51: "(2011)" instead of "(Lignola et al., 2011)".	*This correction was implemented in* ***line 50.***
4	L60: "mode of failure" instead of "failure behavior".	*This suggestion was implemented in* ***line 59.***
5	L68: "Nkurunziza et al. 2005" is not the correct reference (source) for the provided information.	*This correction was implemented in* ***line 68.***
6	L77: define "post-loading".	*This suggestion was implemented by defining post-loading in* ***lines 77-78, 265, 285-286 and 338.***
7	Table 1: How the mechanical properties of the spiral reinforcement was obtained?	*The mechanical properties of the spiral reinforcement were calculated based on the properties of straight bars, as per CSA-S806 (CSA, 2012). This information was added in* ***lines 126-127*** *to respond to the reviewer's comments.* ***Ref:*** CSA 806 (2012). *Design and construction of building structures with fibre-reinforced polymers*, Canadian Standards Association, CAN/CSA-S806-12, Rexdale, ON, Canada.
8	L126: define "post-mixed".	*This suggestion was implemented in* ***line 135.***
9	L139: "… ratio of 2.79% was similar for …".	*This correction was implemented in* ***line 149.***
10	L153: does the 100-mm spiral pitch satisfy the used design code requirement?	*While CSA S806 (CSA, 2012) recommends a clear spacing between spirals of less than 85 mm for the tested columns, the biaxial stress distribution in HCCs compared to the triaxial stress distribution in solid concrete columns (AlAjarmeh et al., 2019) requires that the most effective spiral spacing for HCCs be determined. This information was added in the revised manuscript in*

		lines 161-164 *to answer the reviewer's query.* ***Ref:*** CSA 806 (2012). *Design and construction of building structures with fibre-reinforced polymers*, Canadian Standards Association, CAN/CSA-S806-12, Rexdale, ON, Canada. AlAjarmeh OS, Manalo AC, Benmokrane B, Karunasena W, Mendis P, and Nguyen KTQ (2019a). "Compressive behavior of axially loaded circular hollow concrete columns reinforced with GFRP bars and spirals." *Construction and Building Materials*, 194, 12-23. AlAjarmeh, O. S., Manalo, A. C., Benmokrane, B., Karunasena, W., and Mendis, P. (2019b). "Axial performance of hollow concrete columns reinf orced with GFRP composite bars with different reinforcement ratios." *Composite Structures*, 213(1), 12.
11	Fig. 2: The text (sample designation) is written on separate lines with different line spacing is confusing.	*This correction was implemented in **Fig. 2.***
12	L182: remove "electrical resistance" or add it on L178.	*This suggestion was implemented in **line 195.***
13	L248 and Fig. 5: define "deformation".	*This suggestion was implemented in **line 260-261.***
14	L289: define "second peak" and show it on Fig. 5.	*The reviewer's suggestion was implemented in **Figs. 5 and 9,** and in **lines 291.***
15	Tables 3 & 4: define the different symbols in a footnote.	*This suggestion was implemented by adding a new section that includes all the notations used in this manuscript (see **lines 743-745**).*
16	Figs. 6 & 10: Lines will not print well in black & white.	*This suggestion was implemented. **Figures 6 and 10** were revised by changing the color of all lines to black and white and using different line types.*

<u>Reviewer # 1</u>

The authors are to be commended on a job very well done. The major contribution of this research work is validation that the design-load capacity of GFRP-reinforced hollow concrete columns can be accurately predicted by considering the contribution of the concrete gross section and the longitudinal GFRP bars at 0.003 axial strain. This is an important finding for researchers and practicing engineers. The experimental test matrix is very well thought of and the conduct is sound and very well carried out. The data presentation and discussion is very well done. This is a very good manuscript and I recommend its publication.

Authors' Responses

The authors would like to thank Reviewer#1 for her/his comments that the works presented in the manuscript is very well thought, the data presentation and discussion is very well done, and that the findings from the work will provide significant contribution of the field.

Reviewer # 2

Good Article and revision is suggested.

Authors' Responses

The authors would like to thank the reviewer for her/his efforts and time in reviewing the paper. His comment will surely enhance and add a strength to the paper. In the following table, the authors have attempted to respect and answer the reviewers' comments.

No.	Reviewer's comments	Authors' responses
1	Editorial and sentence formation could be improved throughout the paper by proper sentence formations, e.g., lines 120, 126, 128, 149 and various other locations.	*This correction was implemented in the locations identified (see* ***lines 129, 136-137, 160-161 and 165-166****. The whole manuscript was checked; grammar and language errors were corrected.*
2	Several sentences need intelligent interpretation and if authors explain it with the addition of few words and revisions the meanings will be clear.	*This suggestion was implemented. The whole manuscript was checked; grammar and language errors were corrected.*

3	For example, D.F. in tables implies ductility factor (D.F.) but the readers have to decipher those terms though the term may also mean deformability factor, which is not the case here.	*This suggestion was implemented by adding a new section (**lines 743-745**) providing all the notations used in the manuscript.*
4	Some of the terms such as first peak and second peak should be identified in the figures for clarity.	*This was addressed in the response to **comment 14** by the associate editor.*
5	Meaning of terms such as post-loading behavior in Line 591 and earlier locations is unclear and shouldn't be left to the reader interpretation.	*This was addressed in the response to **comment 6** by the associate editor.*
6	Eqn. (2) is incorrect as provided and needs correction with the signs.	*This correction was implemented in **line 556.***
7	Figures need to be identified with locations of the beginning of confinement activation as mentioned in several instances within the paper.	*This was addressed in the response to **comment 14** by the associate editor. More descriptions of the beginning of the confinement activation were also added in **lines 268-269, 281, and 286.***
8	Terms such as first peak and second peak load need to be identified in figures for reader clarity.	*This was addressed in the response to **comment 14** by the associate editor..*
9	Explanation on use of 0.003 for longitudinal strain in FRP bars for compressive strength calculation is not convincing and needs better supporting explanation.	*Supporting explanation on the use of 0.003 for longitudinal strain in FRP bars for compressive strength calculation was added in **lines 551-553** to clarify the concerns of the reviewer.*
10	Similar to item 10, use of 0.0095 for secondary peak load also needs explanation and the percentage contribution to total compressive strength between the strain of 0.003 and 0.0095 need to be mentioned.	*The explanation on the use of 0.0095 to calculate the secondary peak load can be found in **lines 576-578.** Additional information to support this approach was provided in **lines 583-586.***
11	Lines 602 and 603 need to separately identify the strength and stiffness enhancement ranges since the statement appears to provide confusing conclusion.	*This correction was implemented in **line 623**.*

Reviewer # 3

This paper presents results from an experimental investigation into the effect of spiral spacing and concrete compressive strength on the load capacity and failure behaviour GFRP reinforced hollow concrete column test specimens. At the end of the manuscript the use of a few existing empirical formulae for the prediction of the failure load of the column test specimens is also presented. Despite the paper is well-written and the key information are presented, the paper does not contribute to an advance of the existing knowledge. The major results "reduction of spiral spacing resulted in increase axial load capacity" and "use of high strength concrete increased the load capacity but reduced the ductility " are well known and previously shown by many authors, including the some authors of this paper. The experimental arrangements and the test specimen geometries and reinforcement details are limited to those investigated in the previously published papers. An experimental investigation of different design parameters and column geometries would have been a good objective for this paper. My recommendation is that the paper should be rejected.

Authors' Responses

The authors would like to thank the reviewer for his efforts and time in reviewing the paper. In the following table, the authors have attempted to respect and answer the reviewers' comments.

No.	Reviewer's comments	Authors' responses
1	At the end of the manuscript the use of a few existing empirical formulae for the prediction of the failure load of the column test specimens is also presented. Despite the paper is well-written and the key information are presented, the paper does not contribute to an advance of the existing knowledge. The major results "reduction of spiral spacing resulted in increase axial load capacity" and "use of high strength concrete increased the load capacity but reduced the ductility " are well known and previously shown by many authors, including the some authors of this paper.	*The motivation, objectives, and novelty of the work presented in the manuscript are highlighted in the Introduction. Many significant new findings were discussed and presented, which will provide a better understanding of the behavior of hollow concrete columns reinforced with GFRP bars. These significant contributions were recognized and commended by Reviewers 1 and 2.* *While the reviewer indicated that some existing empirical formulas were used in this study, these formulas were developed for steel-reinforced hollow columns and GFRP-reinforced solid concrete columns. The experimental work and the*

		data obtained from the current work enabled the authors to determine the applicability of these formulas and to modify them to predict the behavior of hollow concrete columns reinforced with GFRP bars and spirals. These developed and proposed new equations were substantially different from the previous studies and contribute new knowledge to the field.
2	The experimental arrangements and the test specimen geometries and reinforcement details are limited to those investigated in the previously published papers. An experimental investigation of different design parameters and column geometries would have been a good objective for this paper.	*The authors acknowledge this comment from the reviewer. The work presented in the current manuscript is a part of comprehensive testing program aimed at gaining a detailed understanding of the effect of critical design parameters on the compressive behavior of hollow circular concrete columns reinforced with GFRP bars and spirals. The results of the significant findings from the research that investigated the effect of cross-sectional configurations (inner-to-outer diameter ratio) and the different reinforcement ratios have now been published in Alajarmeh et al. (2019a) and Alajarmeh et al. (2019b), respectively. These significant findings, which are related to the current paper, were added in the* ***Introduction (lines 93-102)****, and in* ***Specimen Details (lines 161-164 and 170-172)*** *to differentiate the scope and highlight the novelty of the current work.* ***References:*** AlAjarmeh OS, Manalo AC, Benmokrane B, Karunasena W, Mendis P, and Nguyen KTQ (2019a). "Compressive behavior of axially loaded circular hollow concrete columns reinforced with GFRP bars and spirals." *Construction and Building Materials*, 194, 12-23. AlAjarmeh, O. S., Manalo, A. C., Benmokrane, B., Karunasena, W., and Mendis, P. (2019b). "Axial performance of hollow concrete columns reinforced with GFRP composite bars with

		different reinforcement ratios." *Composite Structures*, 213(1), 12.